Project Report
LSP-203

Monolayer Tungsten Disulfide as a Valleytronic Material: FY17 Line-Supported Novel and Engineered Materials Program

S.A. Vitale
D.A. Nezich
J.O. Varghese

2 February 2018

Lincoln Laboratory
MASSACHUSETTS INSTITUTE OF TECHNOLOGY
LEXINGTON, MASSACHUSETTS

This material is based upon work supported by the Assistant Secretary of Defense for Research and Engineering under Air Force Contract No. FA8721-05-C-0002 and/or FA8702-15-D-0001.

DISTRIBUTION STATEMENT A. Approved for public release: distribution unlimited.

This report is the result of studies performed at Lincoln Laboratory, a federally funded research and development center operated by Massachusetts Institute of Technology. This material is based upon work supported by the Assistant Secretary of Defense for Research and Engineering under Air Force Contract No. FA8721-05-C-0002 and/or FA8702-15-D-0001. Any opinions, findings, conclusions or recommendations expressed in this material are those of the author(s) and do not necessarily reflect the views of the Assistant Secretary of Defense for Research and Engineering.

© 2017 MASSACHUSETTS INSTITUTE OF TECHNOLOGY

Delivered to the U.S. Government with Unlimited Rights, as defined in DFARS Part 252.227-7013 or 7014 (Feb 2014). Notwithstanding any copyright notice, U.S. Government rights in this work are defined by DFARS 252.227-7013 or DFARS 252.227-7014 as detailed above. Use of this work other than as specifically authorized by the U.S. Government may violate any copyrights that exist in this work.

Massachusetts Institute of Technology
Lincoln Laboratory

Monolayer Tungsten Disulfide as a Valleytronic Material: FY17 Line-Supported Novel and Engineered Materials Program

S.A. Vitale
D.A. Nezich
J.O. Varghese

Group 81

Project Report LSP-203

2 February 2017

DISTRIBUTION STATEMENT A. Approved for
public release: distribution unlimited.

Lexington Massachusetts

This page intentionally left blank.

ABSTRACT

Both classical and quantum computing face significant challenges. Field effect transistor technology is reaching the fundamental limits of scaling and no proposed replacement technology has yet demonstrated even comparable performance. Scaling the number of entangled qubits to that required to solve useful problems is an enormous challenge with current device technology. Both fields stand to benefit from transformational devices based on new physical phenomena. Two-dimensional transition metal dichalcogenides (TMDs) possess a number of intriguing electronic, photonic, and excitonic properties. This proposal focuses on their valleytronic properties, which are truly unique to this new class of materials. Due to a lack of inversion symmetry and strong spin-orbit coupling, 2D TMDs possess individually addressable valleys in momentum space at the K and K' points in the first Brillouin zone. This valley addressability opens the possibility of using electron and hole momentum states as a completely new paradigm in information processing. Manipulating the K and K' momentum states could permit classical computation at a small fraction of the energy cost incurred by traditional field effect transistors. For quantum computation, qubits could be constructed out of TMD devices, with the benefit of long coherence times at elevated temperatures due to valley-protection of the spin states.

FY17 was the second of a three-year effort to develop the underlying materials, characterization techniques, physical devices, and architectures to enable valleytronic computing. Our intent is to pursue a transformational advance in information processing as opposed to a lower-risk, evolutionary approach, hence the three year timeline. This report covers three areas of work perfomred in FY17. First, a valleytronics workshop was organized which attracted more than 50 of the leading reserachers in valleytronics and related fields. A summary of this workshop is presented first as it serves to put the currnet effort in context. Next is a section on the the growth of wafer-scale valleytronic material with large single-crystal domains. The third section focuses on spectroscopic characterization of key valleytronic properties such as carrier lifetime and valley coherence.

This page intentionally left blank.

TABLE OF CONTENTS

		Page
	Abstract	i
	List of Illustrations	v
1.	INTRODUCTION TO VALLEYTRONICS	1
2.	VALLEYTRONICS WORKSHOP	5
	2.1 List of Participants	6
	2.2 Meeting Organization	7
	2.3 Valleytronics current state of the art, challenges, and opportunities	7
3.	TRANSITION METAL DICHALCOGENIDE GROWTH	17
	3.1 Introduction	17
	3.2 Vapor Phase Epitaxy	18
	3.3 Thin-film precursor vapor phase epitaxy	26
	3.4 TEM Imaging	28
4.	DEVICE FABRICATION AND SPATIO-TEMPORALLY RESOLVED PHOTOLUMINESCENCE SPECTROSCOPY	31
	4.1 Introduction	31
	4.2 Wafer-scale device fabrication	32
	4.3 Spatio-temporally resolved Photoluminescence Spectroscopy	38
5.	PUBLICATIONS AND PRESENTATIONS	41
6.	SUMMARY	43

This page intentionally left blank.

LIST OF ILLUSTRATIONS

Figure No.		Page
1	State of the art and program goals for sample area, domain size, and valley lifetime.	17
2	MIT LL vapor phase epitaxy reactor.	18
3	FY16 growth results: clean and crystalline WS_2.	20
4	FY16 growth results: highest photoluminescent yield WS_2.	20
5	Illustration of reactor modifications.	21
6	FY17 growth results: highest photoluminescent yield WS_2.	22
7	FY17 growth results: full wafer coverage WS_2.	23
8	Layer-by-layer transfer of MIT LL WS_2 films by Jeehwan Kim at MIT.	24
9	AFM imaging of domain boundaries in continuous WS_2 films.	25
10	Modified susceptor assembly used for TFP-VPE growth of MoS_2.	26
11	Characterization of the material produced by two-step TFP-VPE.	27
12	Aberration-corrected TEM Images of WS_2.	29
13	Large-scale MoS_2 device patterning.	32
14	Back-gated MoS_2 transistor.	33
15	MoS_2 transistor transfer characteristic curve.	34
16	Raman spectrum of single-layer MoS_2.	35
17	Single-layer MoS_2 photoluminescence.	36
18	Spatial map of steady-state photoluminescence of single-layer MoS_2.	37
19	Valley-based photoluminescent response of single-layer MoS_2.	38
20	Single-layer MoS_2 spatio-temporal dynamics.	39
21	Custom system time-resolved decay trace.	40

This page intentionally left blank.

1. INTRODUCTION TO VALLEYTRONICS

As traditional charge-based silicon microelectronics reach fundamental performance limits, researchers are exploring new computational architectures and devices to enable further increases in performance and reductions in power. Valleytronics is a potential new computational paradigm which exploits the momentum state of an electron, hole, or exciton as an additional degree of freedom for information processing.

Periodic semiconductor crystal lattices often have degenerate minima in the conduction band at certain points in momentum space. We refer to these minima as valleys, and devices which exploit the fact that carriers are present in one valley versus another are referred to as valleytronic devices. Though degenerate valleys are present in many periodic solids, in most cases it is impossible to address or manipulate carriers in one valley versus another as the valley state of a carrier is not coupled to any external force we can apply. Thus it is not possible to construct valleytronic devices out of most materials. This is in contrast to spintronics, for example, where the electron spin is readily manipulated by magnetic fields through the electron spin magnetic moment or (less easily) by electric fields through spin-orbit coupling.

In some cases, carrier mass anisotropy along different crystal orientations can result in valley polarization; preferential scattering occurs from one valley into another. This has been shown in diamond, aluminum arsenide, silicon, and bismuth at cryogenic temperatures. However these materials still lack a strong coupling between the valley index (sometimes called the valley pseudospin) and any external quantity such as an applied field. It is not clear that there is a way to use mass anisotropy to produce a useful device such as a switch.

The recent emergence of 2D materials has provided a more encouraging space in which to explore manipulation and control of the valley index. 2D materials with hexagonal lattices such as graphene or transition metal dichalcogenides (TMDs) have valleys at the K and K' points in the Brillouin zone. But to detect or manipulate carriers selectively in one valley we need some measureable physical quantity which distinguishes the two. The following discussion which describes valley addressability in 2D hexagonal materials is largely based on the paper from X. Wu, W. Yao, D. Xiao, T.F. Heinz, "Spin and pseudospins in layered transition metal dichalcogenides," Nature Physics, **10**:343 (2014).

The K and K' points are time-reversed images of one another, so in general physical qualities that have odd parity under time reversal are good candidates to distinguish valley states. For example, if the at the K and K' points the Berry curvature and orbital magnetic moment are non-equivalent one can in principle distinguish between the valleys using electric and magnetic fields, respectively. However, if inversion symmetry is also present, it would render both the Berry curvature and orbital magnetic moment vanishing because they are pseudovectors. This is shown below.

It has been shown that the equations of motion for Bloch electrons under applied electric and magnetic fields are:

$$\dot{\boldsymbol{r}} = \frac{1}{\hbar}\frac{\partial E_n(\boldsymbol{k})}{\partial \boldsymbol{k}} - \dot{\boldsymbol{k}}\times\Omega_n(\boldsymbol{k})$$

$$\hbar\dot{\boldsymbol{k}} = -e\boldsymbol{E} - e\dot{\boldsymbol{r}}\times\boldsymbol{B}$$

where Ω is the Berry curvature defined in terms of the Bloch functions,

$$\boldsymbol{\Omega_n}(\boldsymbol{k}) = \nabla_{\boldsymbol{k}}\times A_n(\boldsymbol{k})$$

$$A_n(\boldsymbol{k}) = i\int u_n^*(\boldsymbol{r},\boldsymbol{k})\,\nabla_{\boldsymbol{k}} u_n(\boldsymbol{r},\boldsymbol{k})\,d^3\boldsymbol{r}$$

A_n is the Berry connection and u_n is the periodic part of the Bloch electron wavefunction in the n^{th} energy band. The Berry curvature can also be written as

$$\boldsymbol{\Omega}_n(\boldsymbol{k}) = i\frac{\hbar^2}{m^2}\sum_{i\neq n}\frac{\boldsymbol{P}_{n,i}(\boldsymbol{k})\times\boldsymbol{P}_{i,n}(\boldsymbol{k})}{\left[E_n^0(\boldsymbol{k}) - E_i^0(\boldsymbol{k})\right]^2}$$

Where $E_n^0(\boldsymbol{k})$ is the energy dispersion of the n^{th} band, and $\boldsymbol{P}_{n,i}(\boldsymbol{k}) = \langle u_n|v|u_i\rangle$ is the matrix element of the velocity operator. The Berry curvature describes the geometric properties of the Bloch bands, and is central to the understanding of topological insulators and other band topology related effects. By demanding that the equation of motion must remain invariant under the system symmetry, one can see that with time-reversal symmetry, $\boldsymbol{\Omega}_n(\boldsymbol{k}) = -\boldsymbol{\Omega}_n(-\boldsymbol{k})$, and with inversion symmetry $\boldsymbol{\Omega}_n(\boldsymbol{k}) = \boldsymbol{\Omega}_n(-\boldsymbol{k})$. Thus only when inversion symmetry is broken can valley-contrasting phenomena manifest. We can see that if an in plane electric field is applied in a 2D crystal then a non-zero Berry curvature results in an anomalous electron velocity perpendicular to the field, but the velocity would have opposite sign in opposite valleys.

The broken inversion symmetry also allows the existence of an orbital magnetic momentum. Intuitively, it can be regarded as due to the self-rotation of an electron wavepacket. The electron energy dispersion in the n^{th} band is modified to,

$$E_n(\boldsymbol{k}) = E_n^0(\boldsymbol{k}) - \boldsymbol{m_n}(\boldsymbol{k})\cdot\boldsymbol{B}$$

where the quantity **m** is the orbital magnetic moment, given by:

$$\boldsymbol{m}(\boldsymbol{k}) = i\frac{e\hbar}{2m^2}\sum_{i\neq n}\frac{\boldsymbol{P}_{n,i}(\boldsymbol{k})\times\boldsymbol{P}_{i,n}(\boldsymbol{k})}{E_n^0(\boldsymbol{k}) - E_i^0(\boldsymbol{k})}$$

Finite **m** is responsible for the anomalous g factor of electrons in semiconductors, which manifests itself in a shift of Zeeman energy in the presence of a magnetic field.

Finally, the existence of finite orbital magnetic moment also suggests that the valley carriers will respond differently to circularly polarized light. The physics behind this phenomenon is the same as in circular dichroism whereby in time-reversal broken systems, the optical absorption of left- and right-polarized light is different. This will manifest as a valley optical selection rule.

The 2H phases of 2D transition metal dichalcogenides lack inversion symmetry and as a result exhibit contrasting **Ω** and **m** between the K and K' valleys. The $\boldsymbol{k}\cdot\boldsymbol{p}$ Hamiltonian at the K and K' band edges is given by:

$$\widehat{H} = at\left(\tau_z k_x \sigma_x + k_y \sigma_y\right) + \frac{\Delta}{2}\sigma_z$$

Where a is the lattice spacing, t is the nearest neighbor hopping integral, $\tau_z = \pm 1$ is the valley index, and Δ is the bandgap. In this case the Berry curvature in the conduction band is given by

$$\boldsymbol{\Omega}_c(k) = -\hat{\boldsymbol{z}}\frac{2a^2t^2\Delta}{(4a^2t^2k^2+\Delta^2)^{3/2}}\tau_z$$

Because of the finite Berry curvature with opposite signs in the two valleys, an in-plane electric field induces a valley Hall effect (VHE)for the carriers. Note that the Berry curvature in the valence band is equal to that in the conduction band but with opposite sign.

The orbital magnetic moment has identical values in the valance and conduction bands:

$$\boldsymbol{m}(k) = -\hat{\boldsymbol{z}}\frac{2a^2t^2\Delta}{4a^2t^2k^2+\Delta^2}\frac{e}{2\hbar}\tau_z$$

Non-zero **m** implies that the valleys have contrasting magnetic moments (through $\tau_z = \pm 1$) and thus it is possible to detect valley polarization through a magnetic signature. The orbital magnetic moment also gives rise to the circularly polarized optical selection rules for interband transitions. The Berry curvature, orbital magnetic moment, and optical circular dichroism η(**k**) are related by

$$\eta(\boldsymbol{k}) = -\frac{\boldsymbol{m}(\boldsymbol{k})\cdot\hat{\boldsymbol{z}}}{\mu_B^*(\boldsymbol{k})} = -\frac{\boldsymbol{\Omega}(\boldsymbol{k})\cdot\hat{\boldsymbol{z}}}{\mu_B^*(\boldsymbol{k})}\frac{e}{2\hbar}\Delta(\boldsymbol{k})$$

Where $\mu_B^* = e\hbar/2m^*$ and $\Delta(\boldsymbol{k}) = (4a^2t^2k^2+\Delta^2)^{1/2}$ is the direct transition energy at **k**. At the K and K' points where k=0, we have full selectivity with $\eta = -\tau_z$. This implies that the transition at K couples only to σ^+ light and the transition at K' couples only to σ^-. This selectivity allows the optical preparation, control, and detection of valley polarization.

In summary, if the Berry curvature has different values at the K and K' point one can expect different carrier behavior in each valley as a function of an applied electric field. If the orbital magnetic moment has different values at the K and K' point one can expect different carrier behavior in each valley as a function

of an applied magnetic field. Contrasting values of $\boldsymbol{\Omega}$ and $\mathbf{m}$ at the K and K' points give rise to optical circular dichroism between the two valleys. In order to have contrasting values of $\boldsymbol{\Omega}$ and $\mathbf{m}$ it is necessary that the material exhibit a lack of spatial inversion symmetry, which essentially is possible only in 2D materials, of which the 2D TMDs are the most promising in part due to their direct bandgap at the K and K' points.

2. VALLEYTRONICS WORKSHOP

The Valleytronics Materials, Architectures, and Devices Workshop, sponsored by the MIT Lincoln Laboratory Technology Office and co-sponsored by NSF, was held at the MIT Samberg Center on August 22-23. Valleytronics is an emerging field which promises transformational advances in information processing through the use of a charge carrier's momentum index in conjunction with its charge and/or spin. Isolation of 2D materials such as graphene and transition metal dichalcogenides has allowed realization of experiments confirming the basic properties associated with valley physics. However development of useful devices for valleytronic computing or other technologies requires significant advancements in material quality, device designs, and circuit architectures.

This event gathered the leading researchers in the field to present their latest work and to participate in honest and open discussion about the opportunities and challenges of developing applications of valleytronic technology. The workshop, originally limited to 42 attendees, “sold out” within three days of the initial announcement. This highly successful meeting included 16 invited talks by the most prominent faculty and scientists researching the solid-state physics of valleytronic two-dimensional materials, as well as three interactive working sessions which tackled difficult topics ranging from potential applications in information processing and optoelectronic devices to identifying the most important unresolved physics questions. A poster session allowed students and postdocs to present their latest findings in a relaxed and congenial atmosphere, and to discuss their work with well-known faculty and scientists.

A tangible product of the workshop is a whitepaper which will inform the reader on potential benefits of valleytronic devices, on the state of the art in valleytronics research, and on the challenges to be overcome. We are hopeful this document will also serve to focus future US Government sponsored research programs in fruitful directions.

2.1 LIST OF PARTICIPANTS

Ajit Srivastava, Emory University
Albert Davydov, National Institute of Standards and Technology
Alexander High, University of Chicago Institute for Molecular Engineering
Allan MacDonald, University Of Texas
Andrew Joe, Harvard University
Artem Mishchenko, The University of Manchester
Daniel Gunlycke, US Naval Research Laboratory
Daniel Nezich, MIT Lincoln Laboratory
Di Xiao, Carnegie Mellon University
Dimitris Pavlidis, National Science Foundation
Dominik Wild, Harvard University
Enrico Bellotti, Boston University
Eric Stinaff, Ohio University
Eric Vogel, Georgia Institute of Technology
Fan Zhang, University of Texas at Dallas
Feng Wang, UC Berkeley
Giovanni Scuri, Harvard University
Haidan Wen, Argonne National Lab
Jaejun Yu, Seoul National University
James Hone, Columbia University
Jeffry Kelber, University of North Texas, Dept. of Chemistry
Jie Shan, Penn State University
Jing Kong, MIT
Joe Qiu, Army Research Office
John Schaibley, U Arizona Physics
Jun Xiao, UC Berkeley
Kateryna Pistunova, Harvard University
Kenan Gundogdu, NC State University
Kin Fai Mak, Penn State University
Kuan Eng Johnson Goh, Institute of Materials Research and Engineering
Kyle Seyler, University of Washington
Luis Jauregui, Harvard University
Luiz Gustavo Pimenta Martins, MIT
Marc Ulrich, Army Research Office
Max Lemme, RWTH Aachen University
Nuh Gedik, MIT
Pablo Jarillo-Herrero, MIT
Pani Varanasi, Army Research Office
Philip Hofmann, Aarhus University
Philip Kim, Harvard University
Qi Zhang, Argonne National Lab
Qiong Ma, MIT
Randall Feenstra, Carnegie Mellon University
Riccardo Pisoni, ETH Zurich
Richard Osgood, US Army NSRDEC
Robert Westervelt, Harvard University
Roland Kawakami, The Ohio State University
Scott Crooker, National High Magnetic Field Laboratory
Steven Vitale, MIT Lincoln Laboratory
Suyang Xu, MIT
Tony Heinz, Stanford University
Xiaodong Xu, University of Washington
Yaqing Bie, MIT
You Zhou, Harvard University
Young Hee Lee, Sungkyunkwan University
Yu-Shu Wu, National Tsing-Hua University

2.2 MEETING ORGANIZATION

The meeting was structured to encourage frank discussion and thinking about higher-level topics such as the potential applications of valleytronics, as opposed to narrow technical discussions. Technical talks in the morning were intended to provide intellectual stimulation for the breakout discussions in the afternoon. Talks were not arranged into sessions by topic, instead different topic areas such as theory, material growth, and device measurements were roughly evenly distributed throughout the program to promote cross-connections between different disciplines.

The afternoons were spent in breakout sessions. The attendees were divided into three groups, with the intent to have both theorists and experimentalists in each group. The same groups met for both days. The first day was more free-form and allowed for brainstorming on the topics, whereas day two allowed deeper exploration and crystallization of the emerging ideas. The breakout sessions were charged with providing actionable output on the following three topics: Current State of Knowledge, Emerging Opportunities, and Material, Device, and Architecture Needs.

2.3 VALLEYTRONICS CURRENT STATE OF THE ART, CHALLENGES, AND OPPORTUNITIES

Notes from the collective discussions are being compiled into a whitepaper. The sections which are complete at this time are provided below.

2.3.1 Current State of Knowledge

In this section we consider what has been learned about valleytronics and what are the remaining unanswered physics questions.

The consensus of the group was that the basic valley physics associated with recently observed effects, such as the valley Hall effect, optical circular dichroism, and optical Stark Effect, is understood. However valleytronics is a new field, and many physics questions have not yet been posed, let alone answered.

The unique physics of valleytronic materials stems from lack of inversion symmetry and the ability to address individual valleys by breaking time reversal symmetry through electric and magnetic fields. In fact these characteristics may be used to separate valleytronic materials from other materials which exhibit minima in the band structure. Unfortunately the Zeeman splitting in these materials is very weak, about 0.2 meV/T. Alternatively, it is known that breaking time reversal symmetry through the optical Stark Effect can be done without resorting to extremely high magnetic fields. Other options for creative means to break time reversal symmetry should be further explored.

For valleytronics to be useful, we must also understand the physics of valley transport across a crystalline domain, across domain boundaries, and even between different materials. The physics of valley

transport is not well established and needs study, perhaps through pump-probe experiments with spatially delocalized pump and probe beams.

Just as important as transport is manipulation of the valley state. Though it is known how to create a valley exciton state at any point on the Bloch sphere using circular, linear, or elliptically polarized light, it is not clear how one can manipulate a state once created, such as how to perform a π or $\pi/2$ rotation. Breaking the degeneracy between states by the optical Stark Effect or through other means should cause the phase to evolve differently in the two states thus effecting motion around the Bloch sphere. An actual experimental verification of this would be an important experimental contribution, as would be a theoretical proposal of how one could effect arbitrary transformations. Developing valley analogs of NMR and spin echo techniques would allow the community to leverage the great body of work in these areas to create systems which allow controlled manipulation of valley states.

Valley lifetime and coherence are important topics. There is sometimes confusion between the terms lifetime and coherence; in this section we will use "valley lifetime" or "valley polarization" to mean how long a population of carriers or exciton remains in a certain valley before scattering to another valley. "Valley coherence" is reserved for discussing the phase relationship between particles in two different valleys, such as that induced by linearly polarized light. Valley lifetime is critical as any device which makes use of polarized valley populations will only be useful for a long as that valley polarization exists.

Valley lifetime for direct excitons is quite short, on the order of 10 ps. The dominant mechanism for loss of valley polarization is not known. A theory is that the loss is dominated by the exciton exchange interaction where annihilation of an exciton in one valley results in the formation of an exciton in the opposite valley. If that is the case, then it may be very difficult to construct a useful device based on direct excitons as it is not clear that there is any practical way to discourage this exchange interaction and prolong valley lifetime. Indirect excitons, where the hole is in one layer and the electron is in the other layer of a bilayer stack of 2D materials, show much longer lifetimes on the order of 100 ns. It is believed that in the indirect case, excitons are protected against the exchange interaction and some other mechanism becomes the limit factor for valley polarization. If this other mechanism is defect-driven for example, it may well be possible to increase valley lifetime by reducing material defect density. Thus understanding the mechanisms of depolarization is critically important. The effect of phonons, disorder, and nuclear spins on valley lifetime has not yet been the subject of study. Additionally, what is the effect of reduced dimensionality on valley lifetime? It is possible that 0D or 1D systems will exhibit more favorable lifetime properties.

Valley lifetime for free carriers has been measured to be much longer, as long as 2 us for holes, and somewhat less for electrons. It is believed that the lifetime is smaller for electrons because the smaller SOC in the conduction band results in less spin-protection of the valley state. It is possible that electron and hole valley lifetimes are much longer than for excitons because the exchange interaction is not available for free carriers. But all of the other possible depolarization mechanisms mentioned above must be studied to understand how to prolong free carrier valley lifetime.

Switching now to valley coherence, it is not completely clear if quantum coherence between valley states is even possible when applied to free carriers. Crystal momentum is a continuous variable, and any small perturbation of an electron or hole from k=0 may destroy coherence. Excitons, by contrast, exhibit one bound state for each region in momentum space. So it may be that excitons are of more utility than free carriers for quantum information applications. On the other hand, since excitons are neutral species they are difficult to transport. Trions (an exciton with an extra electron or hole) may be able to satisfy the need for both coherence and transport.

The surrounding materials will have a significant impact on the valley properties. For example, some substrate materials are known to quench photoluminescence. By contrast, inserting a layer of hBN between TMD layers makes the indirect exciton lifetime longer. Designing a suitable substrate that will not interfere with valleytronic properties, or that may even enhance valleytronic properties, is an exciting topic for computational materials science.

It is known that for a given monolayer of TMD material, the conductivity due to the valley Hall effect cannot be easily tuned, and its magnitude is intrinsically linked to the doping level. It is thus difficult to manipulate the valley Hall effect for single-layers of TMDs. Although the lack of inversion symmetry enables valley-specific phenomena to appear in monolayer TMDs, its absence precludes the possibility of easily tuning the valley Hall effect. Inversion symmetry is restored in bilayers of TMD material, and the application of an electric field perpendicular to the in-plane axes can be used to break it. The strong dependence of both the magnitude and polarity of the valley Hall conductivity on the applied field presents a way to electrically tune the VHE in bilayer TMDs. Perhaps bilayers of TMDs may be more readily useful for valleytronic applications.

There are other opportunities in understanding how valleytronic materials can enable advances in other areas which are not as clearly tied to information processing. For example, bilayers of stacked and rotated 2D materials exhibit moiré patterns. These moiré patterns produce periodic potential wells as deep as 160 meV. These may be useful for creating quasi-atomic lattices of excitons which can be employed as arrays of devices for memory or logic operations. It is known that exciton-polaritons can condense into a BEC. If the BECs at given lattice points in the moiré pattern can be made to interact, it may be possible to realize the BEC equivalent of an atom interferometer.

Additionally, the physics of the relationship between valley and superconductivity has not been explored. Though superconductivity in 2D materials has been demonstrated, valley-polarized superconductivity has not been addressed. Normally Cooper pairs would consist of electrons from opposite valleys, but in valleytronic materials the Cooper pairing may be quite unusual. Is it possible to create a new superconducting quasi particle with electrons from the same valley? 2D superconductivity at low electron density as well as superconductivity in Landau Levels has not yet been studied.

Finally it should be noted that valleys other than K/K’ do exist in these materials, such as at the Γ and Q/Q’ points. There has been essentially no study of whether there are interesting valleytronic properties at these points.

2.3.2 Emerging Opportunities

In this section, we consider what the most promising applications for valleytronics are and what the big technical challenges to realize these applications are.

It is immediately apparent that no "killer app" for valleytronics has yet been identified. The general consensus is that until the present time the small valleytronics community has been focused on material growth and valley physics experiments, without more than some passing thoughts about practical devices or systems based on these materials. So it was very important to take time in this workshop to discuss what the useful and practical technology applications of valleytronic materials are.

Using the valley pseudospin as qubit for quantum computing has some very attractive benefits. It should be significantly easier to integrate thousands or millions of valley qubits in a simple planar architecture compared to other modalities such as trapped ions or quantum dots. In addition, spin protection of valleys or valley protection of spin may provide longer coherence times than other unprotected qubit candidates. Finally, small, planar 2D qubits will likely permit much faster gate operation times than other types of qubits. On the other hand, there is the notable concern that large spin-orbit coupling will increase the interactions between the qubit and its environment, thus reducing coherence time. Thus one important challenge in this space is to measure and understand the decoherence mechanisms of valley qubits.

Classical computation is the canonical application for semiconductor devices, and it is apparent that the unique physics of valleytronic materials offer a new computational degree of freedom. In spite of this, a specific enablement of a valleytronic computational element that provides a real-world advantage over silicon CMOS has not yet been proposed. Thus the most urgent technical challenge in this space is to identify a viable valleytronic logic or memory device design. Though an all-valleytronic computational element is perhaps the most forward-thinking opportunity, one must also consider how valleytronics can enhance computational devices based on other physics. By taking advantage of spin-orbit coupling, it may be easier as a first step to consider valley-protected spin-based devices. Using valleytronic materials for spin injection or detection may provide dramatic improvement in the energy efficiency of these operations. valley-protection of spin could increase the spin lifetime and mean free path which is important for information storage and transport. Increasing valley lifetime is a crucial technical challenge to realize these benefits, as is a theoretical framework to understand the upper limits of allowable defect density.

It is important to point out that valleytronics is not just a subtle variation on spintronics. The physics underlying spin-based and valley-based computing is completely different. Spintronic devices typically are conventional charge-based electronics, but with some enhancement of their retention or on/off ratio characteristics provided by a conductivity difference between spin-up and spin-down electrons through some material. Because of this, spintronic devices have yet to demonstrate real-world power and performance advantage compared to conventional silicon CMOS. Valleytronic devices, by contrast, are expected to perform computation through manipulations of the momentum index of electrons, holes, and/or excitons. This implies that the physics limitations will be different from those of conventional charge-based (and by extension spintronic) electronics. Additionally, in 2D TMDs the spin-protected valley lifetime may

be much longer than that which can be achieved in spin-only systems, and thus new architectures not available to spintronics may be possible.

Developing a valleytronic computational technology which meets or exceeds the current state of the art with respect to performance, power, reliability and cost will be a long term effort. As such, it is also useful to consider applications with less complexity that can be realized in the near-term, even if the impact is less broad. One very compelling idea is to use valleytronic effects to develop non-reciprocal optics such as an integrated photonic optical isolator. Optical isolators are a long-awaited missing component in the integrated photonics toolbox. The inherent optical dichroism present in valleytronic materials along with the means to address individual valleys through breaking time reversal symmetry suggest that these materials could be ideally suited to form a microphotonic optical isolator. It may even be possible to construct a gate-tunable isolator that switches direction based on the applied voltage.

One could also take advantage of the optoelectric properties of valleytronic materials to make polarization sensitive detectors. Polarization sensitive optical detection can provide significant operational advantages, including differentiating man-made objects from natural background clutter and generating high-resolution 3D reconstructions from limited data. Full-Stokes polarimeters measure all four components of the Stokes vector, allowing reconstruction of the polarization of the incoming light whether it is circular, linear, or elliptical. Full-Stokes polarimeters have been demonstrated using mechanically rotated optical filters and liquid crystal-based variable retarders. These systems are slow to rotate between different polarizations which causes loss of resolution due to scene movement between image captures. An intrinsically polarization sensitive detector capable of operating at fast frame rates with no moving parts would open new capabilities for space-based imaging and ranging. However there are no photodetectors of which we are aware which are inherently capable of discriminating between left, right, and linearly polarized light, as would be possible with detectors made from valleytronic materials. Technical challenges in this area include improving the efficiency of light absorption and quantifying the ability to discriminate between light of different polarizations.

Along similar lines, one could develop photon emitters which could dynamically switch polarization based on electrical inputs. This could improve the efficiency of single photon emitters for Quantum Key Distribution or other forms of quantum communication including quantum repeaters for long-haul communications. The fidelity of polarized light emission and improvements in quantum efficiency are technical challenges.

2.3.3 Material, Device, and Architecture Needs

In this section we consider what the community needs to do in order to bring forth viable devices and architectures which take advantage of valleytronic properties.

Defect Reduction

Any device which takes advantage of valleytronic properties will be reliant on some persistent population of electrons, holes, or excitons in those valleys. As such the valley lifetime of a material is a critical property. In addition to persistence, useful devices will likely need to transport electrons, holes, or excitons from one spatial location to another without undue loss of valley information. This implies that valley mean free path or valley scattering length will also be very important. Therefore when we speak of valleytronic quality material we mean that the material possess sufficient valley lifetime and mean free path to perform some function.

Although the community is still in the early stages of understanding this topic, it is plausible that valleytronic properties will be adversely affected by crystal defects. Vacancies, substitutions, and grain boundaries will all play a role. Donor defects (chalcogen vacancies or excess metal atoms) and acceptor defects (metal vacancy or excess chalcogen atoms) are known, but what are the other important defects in TMDs? Once identified, understanding the impact of point and extended defects is essential in order to improve valleytronic properties.

Reducing defect density through improvements in growth processes is of paramount importance. The defect density of common TMDs such as MoS_2 by grown by VPT or CVD is on the order of 10^{13} cm^{-2}. This is roughly 10,000x higher than the defect density in common electronic materials today. Developing better understanding of the chemical kinetics of TMD growth by CVD or other means such as MBE, ALD, or the flux method will allow reduction of defect density.

But what defect density is good enough? This can only be answered concretely in the context of a given device architecture, as will be discussed in a subsequent sub-section, though it has been proposed that valley polarization is linearly proportional to the defect density. For now, it is recommended that the community engage in materials benchmarking and standardization to produce "valleytronic grade" materials with defined properties which include defect density and type(s), carrier concentration, carrier mobility, and photoluminescence. These will serve as proxies for the more critical (and much more difficult to measure) properties of valley lifetime and mean free path.

Dopant density in these materials must be better controlled, and eventually the dopant density must be selectable based on the device needs. Currently, material grown in different laboratories can have widely varying dopant density. In some cases, a material can even exhibit either n-type or p-type behavior between different research groups. It is likely that the substrate material, process cleanliness, and other subtle variables are important here. Maturation of growth processes and protocols is necessary to control dopant density.

Though exfoliation is not expected to be a scalable technique for practical device fabrication, continuing to work with exfoliated material has significant value. Exfoliated material in some cases is more readily prepared as large crystals compared to grown material. One can still study the effect of defects in exfoliated samples, and perform experiments on defect reduction through annealing in chalcogen ambients,

for example. Multilayer stacking of materials can also be performed to study the influence of interfaces, contamination, and layer alignment on valleytronic properties.

Ultimately though, one would like to turn to synthetically grown material for practical applications. Development of TMD growth on industrially important substrates (e.g., sapphire, SiC, Si) with controlled epitaxy, grain size and grain boundaries, and point and extended defect density is important. Monolayer 2D TMDs are still a relatively new class of materials, and one aspect which has not yet been studied is what are the theoretical minimum limits of defect density. An effort to determine the thermodynamic limits of defect density, combined with the effect of those defects on valley lifetime and mean free path, would provide very compelling evidence on the ultimate potential of valleytronic materials.

In the near term, devices built on monolayer 2D materials will have to contend with grain boundaries. Although there have been several reports of "wafer-scale" TMD growth, it should be recognized that this material should properly be called polycrystalline. Understanding diffusion of valley information across grain boundaries will help inform if valleytronic devices are possible on such polycrystalline material, or if single domain films are really required. Concurrently, increasing the grain size of wafer-scale growth methods should be pursued.

Material characterization requires accepted electrical test devices. In addition to Hall bars and van der Pauw structures, more work needs to be done to perfect valleytronic property test structures. These include non-local valley Hall effect devices for valley diffusion and other combined electro-optic test structures for Kerr effect and electroluminescence measurements.

New Materials

The list of 2D materials which have been experimentally realized continues to grow. From a valleytronics perspective, not all of these new 2D materials are clearly useful, however. 2D materials with improved valley lifetime and mean free path are definitely needed. Synthesis of such material by trial and error is likely to be very labor intensive, especially as one begins to consider binary and ternary alloys. A materials modeling effort to design the next generation of valleytronic material would be extremely valuable. Basic questions remain unclear, such as: Will alloys of TMDs retain (or enhance) valleytronic properties? Can we design 2D materials with larger spin orbit coupling and thus greater spin protection of the valley state? Or can we design materials with significant spin orbit coupling in the conduction band as well as the valance band?

One can also look for design principles to guide development of new valleytronic materials. For example, are there trends among the chalcogens (S, Se, Te) to guide us? Or is valleytronics practical in another class of materials beyond 2D hexagonal honeycomb lattices? The community would benefit from a concerted effort in computational materials design to optimize valleytronic properties, starting with TMD and other van-der-Waals layered materials and extending to novel low-dimensional heterostructures such as oxides, nitrides and mixed phases.

In parallel with modeling results it would be useful to create a materials database to combine data from modeling and experimental results focusing on valleytronic properties. Conceivably one could use machine learning or other data mining techniques to discover promising paths for material development.

Valleytronic Devices and Architectures

One can state fairly confidently that there have been no valleytronic devices yet constructed which yields real technology advancements for practical systems. This is a critical gap in the arguments for valleytronics as a practical technology element as opposed to an interesting physics phenomenon. The previous section provided several high-level ideas for valleytronic information processing and novel optoelectronic elements. But fully-developed concepts of how one would actually realize such devices is lacking. Efforts to rectify this situation should be given the highest priority. There is great precedent for device designs which emerged after discovery of new, enabling physical phenomena, such as the discovery of the giant magnetoresistance effect in 1988; valleytronics is just in the incipient stages of developing these ideas. But without concreate device concepts it will be impossible to migrate valleytronics from an obscure physics phenomenon to a broadly studied field with the potential for non-scientific impact.

Though we should not at this stage limit the creativity of investigators to come up with new valleytronic devices concepts, there are several ideas which are of interest to the user community. First is a logic device which uses valleytronic information to gain some advantage over classical MOSFETs. This could include using valley polarizability to enable a sub 60 mV/decade switch, using valley-protection to enable robust room-temperature spin-based computing, or using the momentum index itself to perform computation. Second, a valley-protected spin-qubit or pure valley-qubit design for quantum operations would be of value. Finally, devices for chiral light emission or detection with power or performance advantage over existing commercial technologies should be further developed, for example spin-lasers. Devices need not be composed of only one material, for example the low mobility inherent in TMDs could be circumvented by using graphene interconnects if one can solve the problem of transporting valley information between the two materials. Perhaps this can be done through a clever device design which converts valley information into the spin domain, and back again.

For some of these devices fundamental elements such as how to create valley current gain to allow cascading of devices will be needed. A clear notion of how to flip or otherwise manipulate the valley index is important for others. It should be emphasized that for many applications (perhaps excluding quantum computing) near room temperature operation is a practical requirement.

There exists some work on theoretical constructs for building blocks of these devices. Moiré patterns in twisted heterostructures induce potential wells up to 0.2 eV deep and could allow spatial localization of valleys. At a line defect, it has been shown that asymmetric wavefunctions in these materials go to zero, so density of states goes to zero and thus transmission equals zero. By contrast for symmetric states transmission is 1. This allows valley polarization by using line defects as a filter. Alternatively line defects could be used as physical barriers, to confine transport between two parallel defects.

There is substantial room for improvement in device process development for 2D materials. It has been shown that metal contacts to TMDs and graphene deposited in UHV conditions are far superior to those formed under other conditions. But the choice of metal to deposit for ohmic contact to any given TMD is not clear. Inserting an hBN layer between the metal and the 2D material was shown to improve contract resistance, though this adds significant fabrication complexity. Developing recipes for TMD contacts which do not require heroic efforts would benefit researchers currently struggling with device measurements. It has also been suggested that gate-defined device boundaries edges produce better quality measurements than edges defined by lithography and TMD etching, but more work needs to be done on this topic.

This page intentionally left blank.

3. TRANSITION METAL DICHALCOGENIDE GROWTH

3.1 INTRODUCTION

The goal of the material growth component of this program is to produce high-quality monolayer transition metal dichalcogenide (TMD) films that can be used for valleytronic device fabrication. The improvement of material growth techniques is necessitated by two requirements for the realization of valleytronics: optimization for long valley polarization lifetimes of charge carriers in the TMD material (which is the key property for employing valley physics for information processing), and amenability to scaling (which is necessary for future integrated device production). Assessing scalability is straightforward and can be demonstrated by measuring domain size and distribution across a wafer, but the direct measurement of valley polarization lifetime is difficult and requires specialized equipment. Typically, proxies for valley polarization lifetime are used to inform material growth. The most common proxies are the domain size (which captures macroscopic crystalline order) and the photoluminescent yield (which indirectly measures atomic-scale order since defects such as vacancies may act as dark recombination sites, and is therefore expected to first order to vary proportionally with valley polarization lifetime), though often these proxies are directly related and domain size can be taken as a primary proxy. The goals of material growth as related to the proxy of domain size are illustrated in Figure 1: a uniform TMD film covering a 1 cm^2 area that is sufficient for large integrated circuit fabrication, and a valley polarization lifetime of 10 µs which should be sufficient to allow 10^3 gate operations per bit and therefore enable error-corrected valleytronic computing.

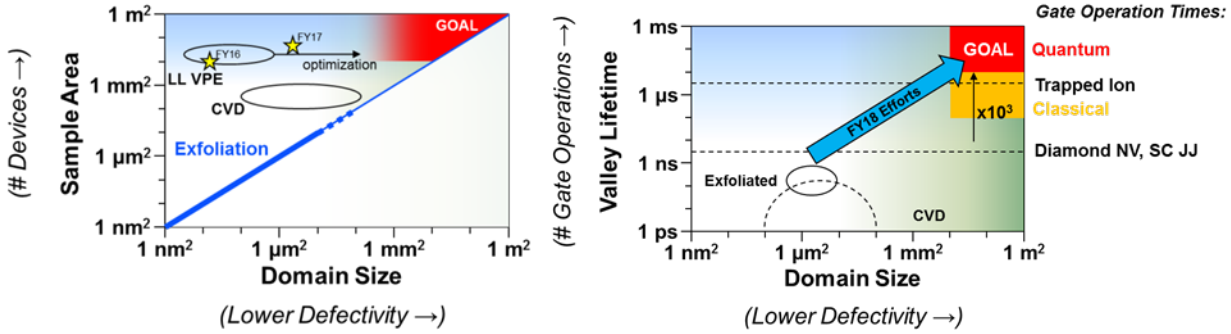

Figure 1. State of the art and program goals for sample area, domain size, and valley lifetime. Relation of critical material metrics (sample area, valley lifetime) to the primary proxy of domain size, with indicated goal of 1 cm^2 sample area and 10 µs valley lifetime.

In the current state of the art, most studies of valley physics are performed on monolayer materials produced by micromechanical cleavage of bulk minerals, which are generally accepted to have the highest available crystallinity, and therefore presumably the longest valley coherence times. However, micromechanical cleavage is not scalable, being limited by its sparse (e.g., 1-10 cm^{-2}) and stochastic

deposition of small monolayers (e.g., 5-50 µm), as well as by the quality and uniformity of the parent crystals and the cleavage and inspection techniques. Other material production techniques are more scalable, such as vapor phase transport (VPT) which grows bulk crystals suitable for micromechanical exfoliation over a period of weeks to months, or which in a short period of time can produce isolated grains or monolayers (e.g., 50 µm grain size, 100µm density uniformity length scale), though this technique is limited as a batch process and has not yet been demonstrated to be capable of stoichiometric tailoring or direct heterostructure growth. Another popular growth method is chemical vapor deposition (CVD) where material is grown from solid precursors in a hot-wall reactor, capable of producing relatively large grains of material (100 µm) and of achieving monolayer coverage, but with significant run-to-run variability due to variations in the solid precursor distribution and reactor geometry. The CVD approach also has difficulty in scaling with the maintenance of uniform temperatures and precursor concentrations.

3.2 VAPOR PHASE EPITAXY

This program employs a variant of CVD using only vapor-phase precursors in a cold-wall reactor, termed vapor phase epitaxy (VPE), with expected benefits to cross-wafer uniformity, controllable stoichiometry, and capability to extend to direct heterostructure growth in the future. The reactor takes 2" wafers in an inductively heated horizontal laminar flow geometry, and employs H_2S gas and vaporized WCl_6 reactants for growth of monolayer WS_2 (Figure 2). The reactor was built in FY15, produced initial results in FY16, and has refined the growth process in FY17. Improvement of grown material quality is indicated by the stars in Figure 1.

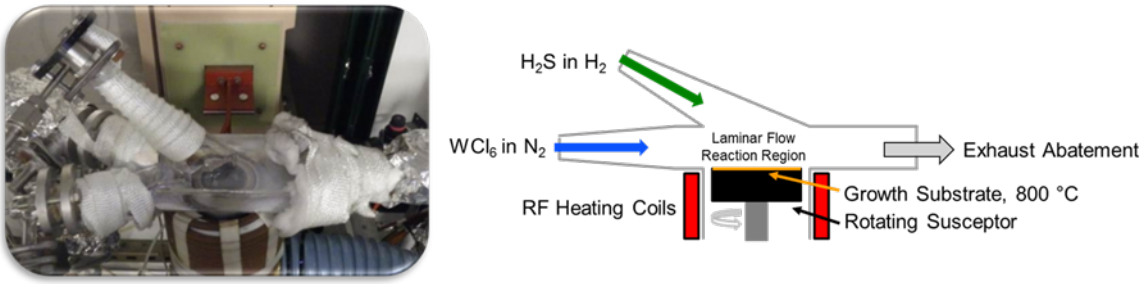

Figure 2. MIT LL vapor phase epitaxy reactor. (Left) Picture of the system as installed. (Right) Illustration of the reactor geometry.

Specifically, the state of growth at the end of FY16 is shown in Figure 3 and Figure 4. These figures display the typical proxy characterizations of domain size (determined by AFM) and photoluminescent yield (mapped over the entire wafer surface, and presented as photoluminescence per unit area). Figure 3 displays characterization for the most crystalline sample produced. In the AFM images, parallel terrace lines of the sapphire substrate are clearly visible, with 0.2 nm height step. Triangular WS_2 flakes are also seen and have typical dimensions of 50 nm at X = 1, 5, 10, 15 mm and 150 nm at X = 20, 25 mm with step heights of 0.6 nm. The variation across the wafer is due to gradients in precursor concentration (highest at

X = 25 mm) and temperature (highest at X = 1 mm) resulting from the specific nozzle geometry of the reactor. A transition is clearly seen from isolated domains of WS_2 at X = 1, 5, 10 mm to a partially merged monolayer of WS_2 at X = 15 mm to a fully merged monolayer of WS_2 at X = 20, 25 mm with larger triangular domains on top (adlayers). The larger domain size of adlayers is due to the altered reactant mobilities and surface energies on the bare sapphire versus a monolayer WS_2 film. There is a strong alignment preference for the WS_2 domains on the sapphire substrate which is propagated up to adlayers, an intended feature of the substrate which we employ to increase the long-scale crystallinity of a merged film and to attempt to eliminate domain boundaries. The photoluminescent signal is strongest for the merged monolayer film, with a typical peak wavelength of 626 nm which is somewhat redshifted from the literature value of 620 nm. Figure 4 displays characterization for the sample with highest photoluminescent yield. The domain size obtained by AFM is larger than in Figure 3 but the domains are more irregular and there is significant particle and nanotube growth across the wafer. The photoluminescent yield is larger and more uniform than in Figure 3, corresponding to the merged monolayer regions at X = 15, 20 mm, with a typical peak wavelength of 620 nm. Variation of peak wavelength for all runs occurred in a range of 612 to 635 nm, but with low enough intensity and reproducibility that attribution for this variation could not be made, though the likely cause is nonstoichiometric vacancy or adatom doping or strain generation due to thermal expansion mismatch, lattice mismatch, or domain merging.

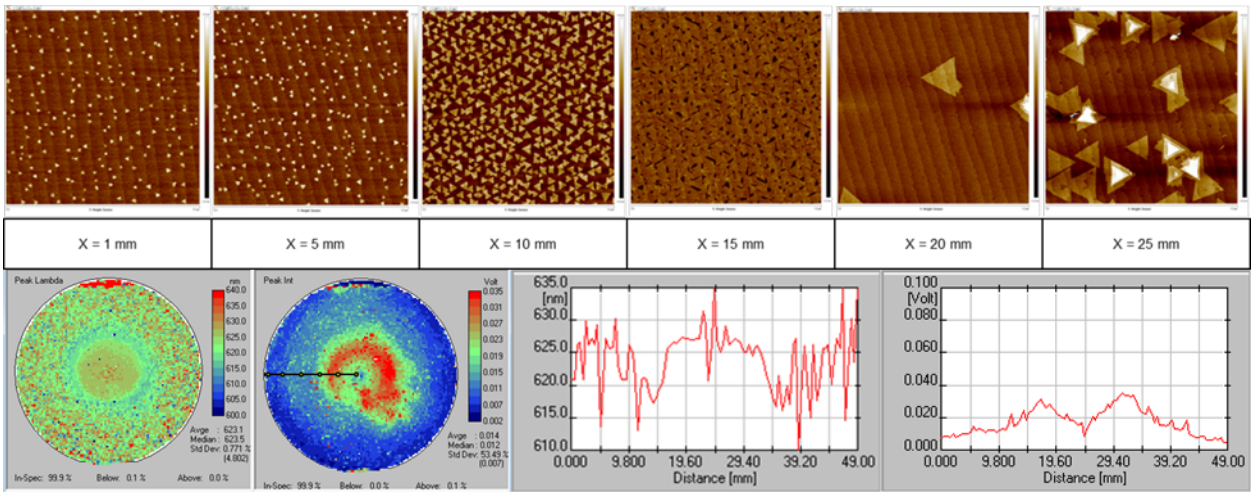

Figure 3. FY16 growth results: clean and crystalline WS_2. (Top) AFM images from across a 2" sapphire wafer. Positions are listed as a distance from the edge of the wafer toward the center of the wafer. Scan size is 1 µm square. Height steps show terraces in the sapphire surface (parallel lines, 0.2 nm height step) and WS_2 domains (triangles, 0.6 nm height step). (Lower Left) Maps of photoluminescent peak wavelength and peak intensity using 532 nm excitation. The black line with yellow dots on the peak intensity map indicates the locations at which the AFM images were acquired. (Lower Right) Line profiles of the photoluminescent maps at (Lower Left), showing peak wavelength (left) and peak intensity (right) along a horizontal line across the wafer. (Run 111)

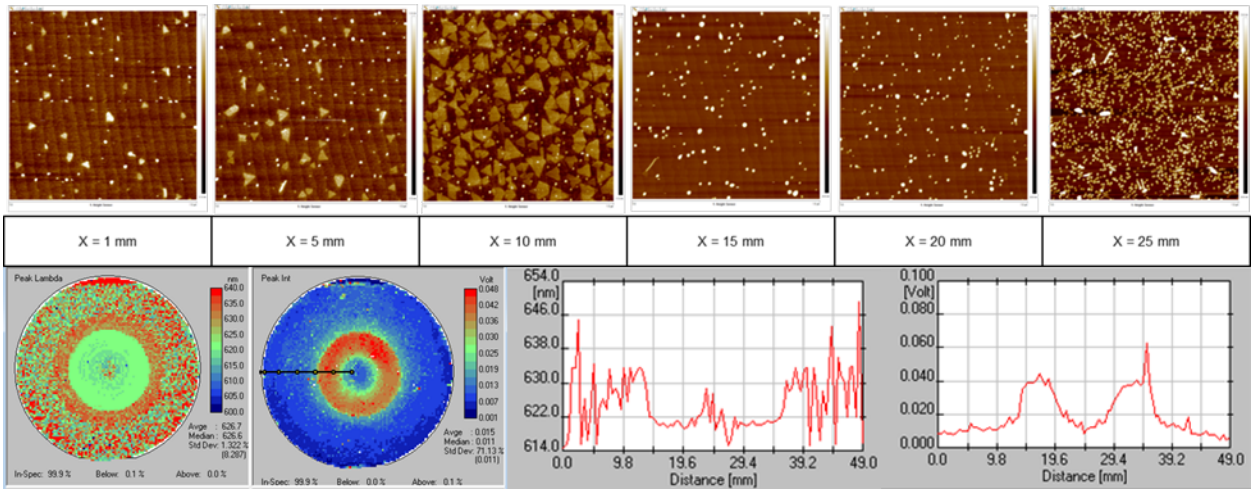

Figure 4. FY16 growth results: highest photoluminescent yield WS_2. Image descriptions are as for Figure 3. (Run 129)

In FY17, we continued to develop our growth process using the VPE reactor. Two major system upgrades added capabilities this year. First, a heated bubbler enclosure system was constructed to ensure uniform precursor delivery to the rector chamber, resulting in improved process repeatability. Second, the chalcogenide gas precursor was changed from a 1% mixture of H_2S in balance of H_2 or N_2 to instead be 100% H_2S which could be diluted within the reactor to any desired concentration with any desired mixture of H_2 and N_2, allowing a much wider process space to be explored. A third major upgrade is in progress with anticipated completion in FY18Q1, consisting of conversion to a downflow reactor geometry and low pressure operation (5-150 Torr) which will allow improved reactant delivery and surface diffusion which is important to further uniformity improvements in temperature and precursor concentration. The major system changes are illustrated in Figure 5.

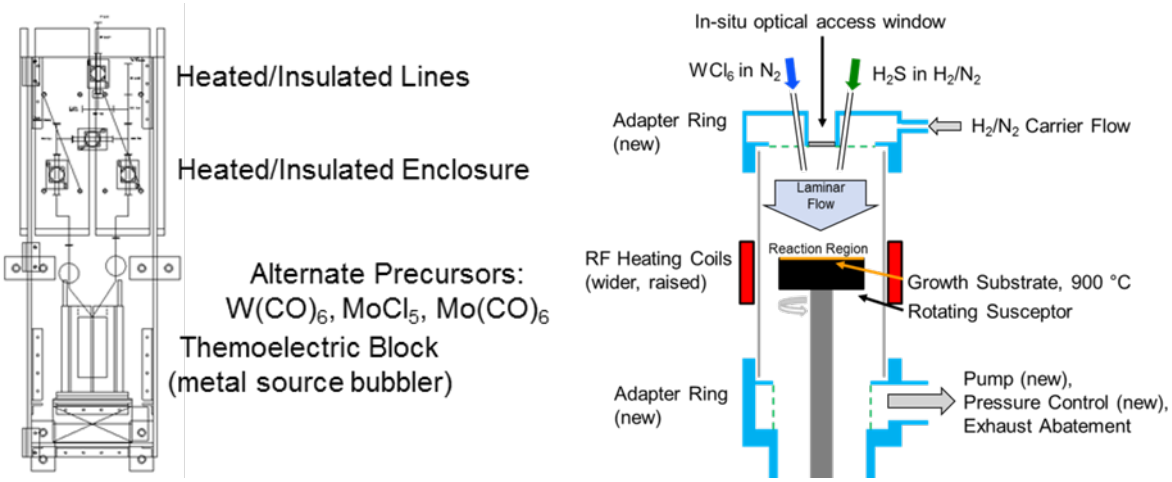

Figure 5. Illustration of reactor modifications. (Left) Schematic for the heated bubbler enclosure implemented in FY17. (Right) Illustration of the reactor conversion to a low-pressure downflow configuration that is underway and scheduled for completion in FY18Q1.

In FY17 we have improved the domain size (5-20x), photoluminescent yield (5x), and wafer coverage (5x) of our films grown by VPE. This was enabled by the transition to 100% H_2S precursor. Further improvements are expected even before the low-pressure downflow conversion, as we are still exploring the process space enabled by the process gas transition. Figure 6 shows a film with high photoluminescent yield (5x that of Figure 4) over a broad region of the wafer, despite being a mostly discontinuous film, with larger grain sizes (up to 500 nm, 5x that of Figure 4) with increased wafer coverage. There are a couple notable features. The ring of high photoluminescent yield is a result of the nozzle geometry of the current reactor, which will be remedied by the low pressure downflow reactor conversion in the coming months. There is also reconstruction of the sapphire terraces during growth to avoid passing beneath the WS_2 domains (particularly obvious at X = 5, 10 mm), which is highly unusual for a low-temperature (<950 C) reactor, and possibly facilitated by the strong reducing atmosphere at the high H_2S concentrations (20%) used for this growth. Such reconstruction implies a strong substrate-WS_2 interaction and heightened

sapphire component mobility which should be explored in the future for how it may affect the epitaxial WS_2 alignment. The domains of this film are less triangular and have a noticeable dendritic component, which should be mitigated by the transition to a low pressure reactor where the surface diffusion length and boundary layer transport are increased. In Figure 7, a three-step growth was employed to sequentially increase the precursor concentration and cover the entire wafer with a WS_2 film (20 cm^2). The photoluminescence intensity profile shows a different correlation with the AFM images than the wafers discussed in the previous figures. Namely, AFM shows a relatively smooth surface interrupted only by bunched sapphire terraces and the WS_2 forms a smooth film over the top of these terraces, so the explanation for this double-ring photoluminescence structure is that the number of WS_2 layers on the wafer varies. Monolayer WS_2 has strong photoluminescence, which is suppressed when there is more than one layer due to the transition to an indirect bandgap as the number of layers is increased. However, in a polycrystalline, multilayer film the adjacent layers may be crystallographically registered or turbostratic, that is, electrically coupled or independent, resulting in suppressed or prominent photoluminescence as they resemble multilayer or monolayer crystallographic structures respectively. This is location dependent, with single layer around the perimeter of the wafer showing prominent photoluminescence (X = 1 mm), with the next ring of suppressed photoluminescence due to growth of a highly-registered second layer (X = 2–10 mm), the next ring of enhanced photoluminescence due to a more turbostratic third layer (X = 10–15 mm), another ring of suppressed photoluminescence that is a return to two highly-registered layers (X = 15–20 mm), and an innermost ring that once more shows increased photoluminescence due to a single monolayer (X = 20–25 mm). The large domains at the wafer edge (up to 2.2 µm, 4x larger than domains across the general field of the wafer) indicate that we are close to drastically increasing our WS_2 grain size through exploiting this beneficial edge proximity effect of temperature and boundary layer thickness directing for process development as we enter FY18.

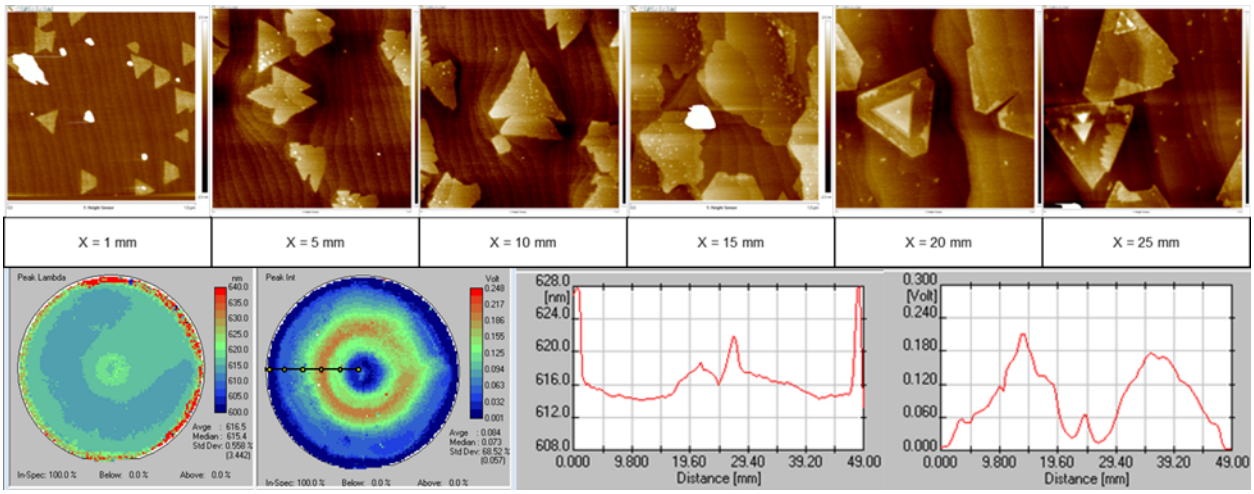

Figure 6. FY17 growth results: highest photoluminescent yield WS_2. Photoluminescence is 5x higher than that of Figure 4 and with a broader luminescent area. The most highly luminescent films have a peak wavelength around 614 nm, smaller than the typical 620 nm observed for WS_2 films produced by other growth techniques. Image descriptions are as for Figure 3. (Run 226)

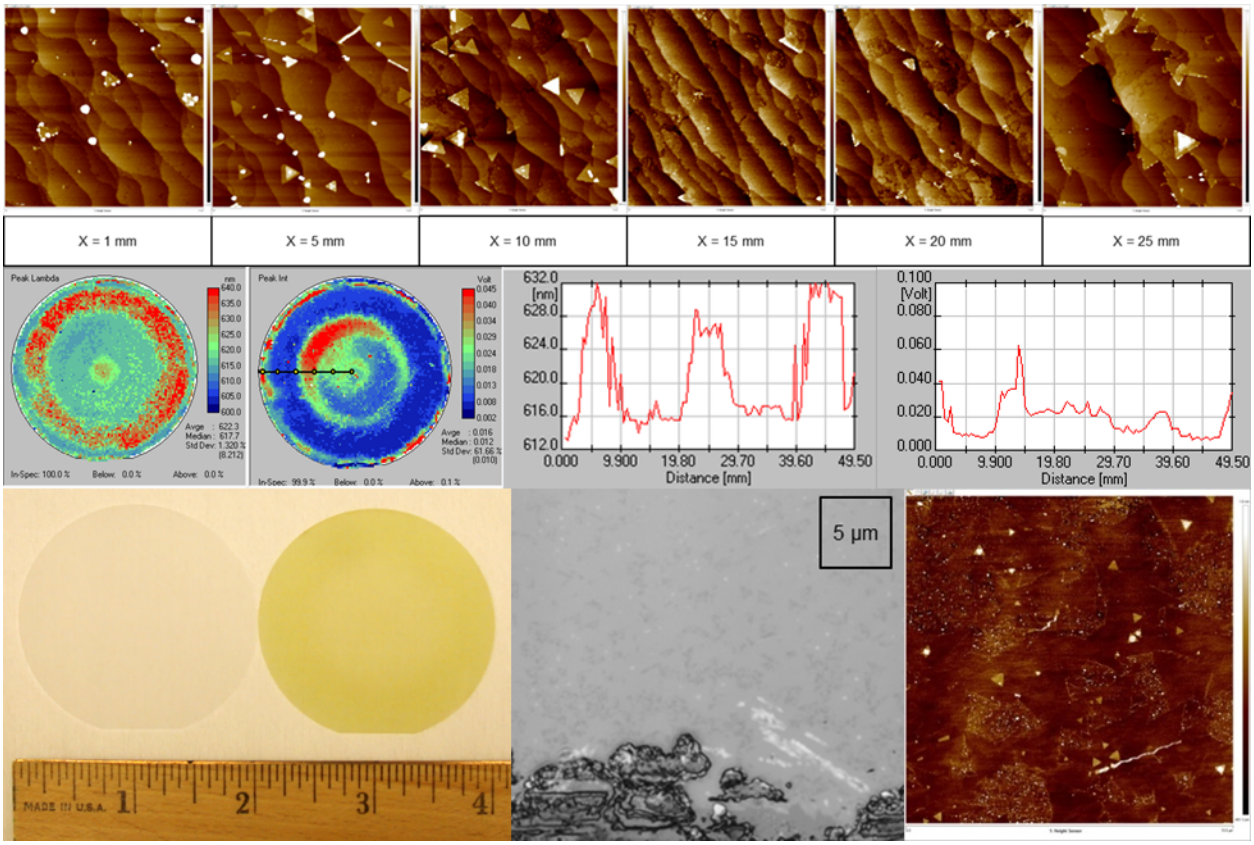

Figure 7. FY17 growth results: full wafer coverage WS_2. Top and middle image descriptions are as for Figure 3. (Bottom Left) Side-by-side picture of a white sapphire wafer before growth and a sapphire wafer with full coverage of yellow WS_2 film. (Bottom Center) Laser reflectance image of the edge of the wafer, showing a partially discontinuous region of WS_2 that has triangular grains up to 2.2 µm long that show as faintly brighter regions. (Bottom Right) AFM scan of the same region in (Bottom Center) showing smooth triangular regions of large domain size connected by rougher regions with many small domains. Scan size is 10 µm. (Run 211)

While the wafer coverage shown in Figure 7 is accompanied by a variation in number of layers, there are two ways in which this growth result is beneficial for valleytronics. First, it is likely that bilayers of TMD materials are desirable for device fabrication because their inversion symmetry can be broken by an applied out-of-plane electric field, resulting in the ability to turn on and off the valley-specific response of these materials. Second, new techniques are being developed which can exfoliate individual monolayers (or generally, n-layers) from multilayer films at the wafer scale, resulting the ability to isolate TMD monolayers with larger grains (and higher quality) that grow on top of the more defective initial layer that is in contact with the substrate (see the discussion of adlayers with respect to Figure 3). This technique is important because it solves the longstanding issue of isolating monolayer films from multilayer films at the wafer scale, while at the same time eliminating the material growth requirement of producing a single

monolayer with all the ensuing complications of substrate interaction. These are huge advances in capability and growth process space.

This second approach has been pursued in FY17Q4, as the full-wafer-coverage multilayer films shown in Figure 7 became available, through collaboration with Professor Jeehwan Kim at MIT. Professor Kim's technique uses stressed metal films as adhesive layers to peel up all of the WS_2 from a wafer and then selectively peel off individual monolayers, which can be transferred to new substrates and analyzed independently. Figure 8 illustrates this layer-by-layer transfer technique, and how it has been used to isolate an individual WS_2 layer from our multilayer films. This initial work is being extended for publication in FY18Q1.

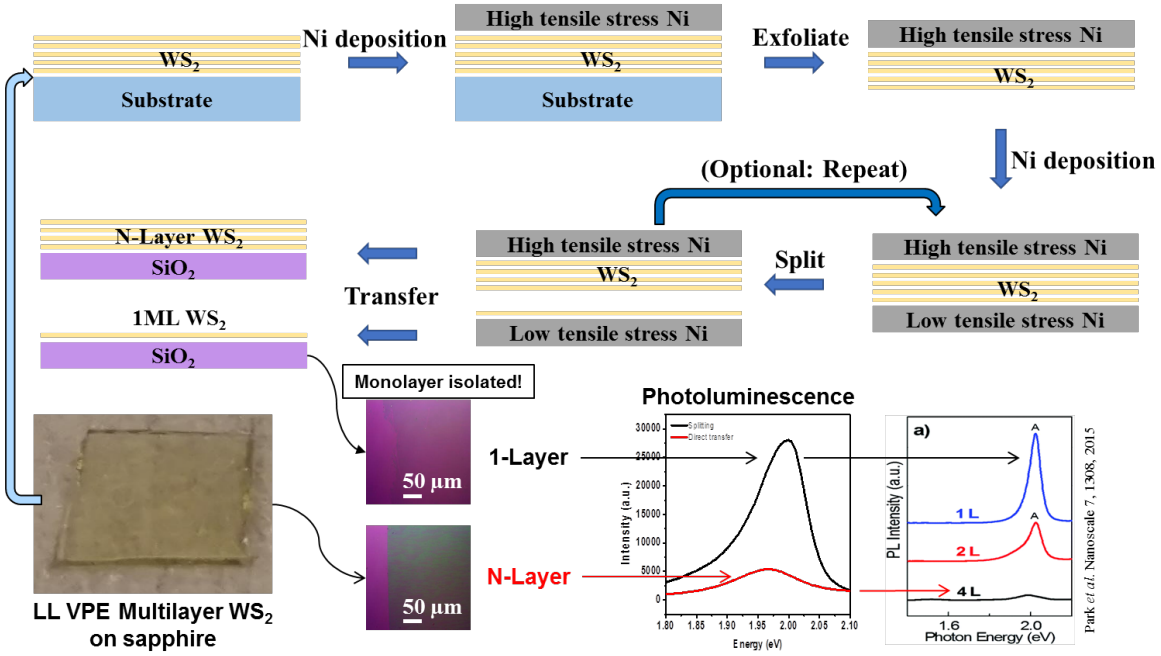

Figure 8. Layer-by-layer transfer of MIT LL WS_2 films by Jeehwan Kim at MIT. Monolayers have been isolated showing a greatly increased photoluminescent yield as expected for monolayer versus multilayer films.

Several general lessons have been learned regarding WS_2 growth that have proven useful in guiding growth process development and that are expected to be applicable to the low-pressure downflow reactor configuration that will be employed in FY18: 1) Domain boundaries can occasionally be imaged by AFM (as in Figure 9). This unexpected and unique ability to image grain boundaries in continuous monolayer films is tip- and scan-dependent, and likely relies on an uncontaminated AFM tip being able to image water that preferentially adsorbs on TMD grain boundaries that have some minimum linear concentration of defects. 2) The reactor's top nozzle purge flow greatly affects the precursor distribution on the wafer, with more flow distributing the precursors more evenly across the wafer but also diluting the precursors and

decreasing their residence time. The optimal flow for the current reactor configuration is 50% of the maximum flow. 3) Higher metal precursor concentration results in a lower nucleation density and therefore a larger domain size, a counterintuitive result that may be specific to the currently employed regime of metal-rich growth. 4) Lower wafer temperature enhances dendritic WS_2 growth, becoming pronounced below 950 °C susceptor temperature for large (>100 nm) domains. 5) WS_2 nanotubes are formed in a narrow window of moderate H_2S concentration, so their presence is a guide that optimal H_2S concentration is at least a factor of two higher than the given conditions. 6) Excess hydrogen leads to large variation in the domain sizes and increased particle formation (see Figure 7 and Figure 9), but some hydrogen concentration is required for growth. The optimal hydrogen concentration in the chalcogen nozzle is currently 20–40%. 7) Higher H_2S concentration results in larger domain size. The most recent growths have already produced 500 nm domains with 20% H_2S concentration, and the limit of this effect is currently being sought. 8) Photoluminescence of small isolated domains (<100 nm) is suppressed, but is recovered as the domains merge to form a continuous film. This let us infer that domain boundaries in a continuous film provide less opportunity for dark exciton recombination than similar densities of domain edges. This is a new result and a first step toward understanding the effect of domain edges and domain boundaries on valley population lifetime.

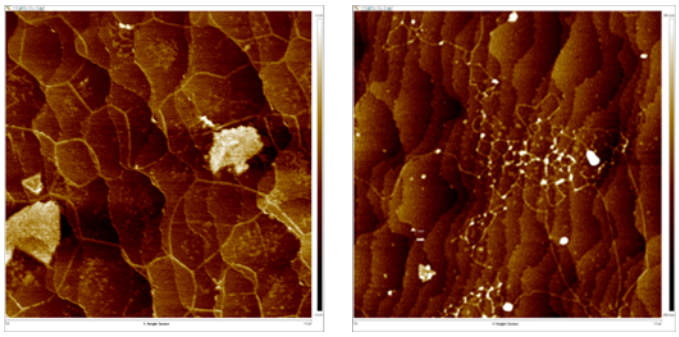

Figure 9. AFM imaging of domain boundaries in continuous WS_2 films. The yellow lines outlining convex areas are the domain boundaries. (Left) A growth condition with optimized hydrogen concentration shows relatively large and uniformly distributed domains (Run 208). (Right) A growth condition with excess hydrogen shows regions of both large and small domain size (Run 224). Scan size is 1 µm square. Color scale is roughly 2 nm.

VPE growth of WS_2 will continue in FY18, using the above results as guides for the new low-pressure downflow configuration. The FY17 goal of decreasing particulates during growth was achieved, but increasing domain size by two orders of magnitude from 100 nm to 10 µm was not achieved – only 1.3 orders of magnitude increase (maximum 2.2 µm domain size) was obtained. Reactor modifications that are in progress are expected to allow completion of this FY17 goal and the FY18 goal of 100 µm domain size in early FY18, with the added benefit of greatly-improved cross-wafer uniformity. Two further extensions of growth technique are planned for FY18: plume-defined growth which is an extension of the technique used to produce full-wafer coverage to small scales which will allow additive growth of WS_2 and ultimately growth of large single-crystal domains of WS_2, and introduction of alternative metal precursors to grow

WS_2 and MoS_2 (currently the TMD species best suited to direct valley polarization lifetime measurements on available tools).

3.3 THIN-FILM PRECURSOR VAPOR PHASE EPITAXY

In addition to the VPE growth of WS_2, a variant method of TMD growth was devised and implemented as a potential alternate route to growth of uniform wafer-scale TMD films. Called thin-film precursor vapor phase epitaxy (TFP-VPE), it is conceptually midway between CVD and VPE in that it uses a thin metal oxide film (e.g., MoO_3) as a highly uniform metal source (as opposed to a metal oxide powder as used in CVD) that is thermally vaporized and transported across a fixed and uniform distance to a growth surface where it can be reduce by a chalcogen hydride gas (e.g., H_2S) to produce monolayer films. A schematic for the modified susceptor assembly fabricated for use in this process is shown in Figure 10.

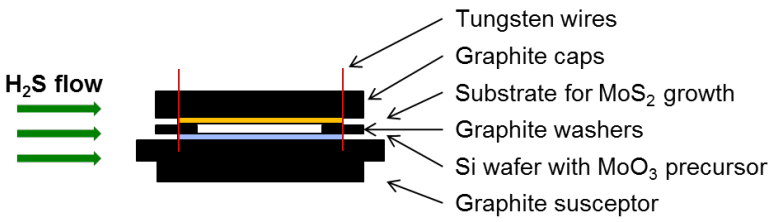

Figure 10. Modified susceptor assembly used for TFP-VPE growth of MoS_2.

The TFP-VPE growth process was implemented using MoO_3 deposited by plasma-enhanced atomic layer deposition (ALD) using the newly-installed Ultratech tool in E-Lab, with the reaction taking place in the VPE reactor in a $H_2S/H_2/N_2$ atmosphere. This involved characterization and optimization of the ALD deposition in order to obtain a uniform film. Preliminary results indicate success using a two-stage growth process, first transporting MoO_3 from the source to the growth target substrate in the absence of hydrogen, and second sulfurizing the MoO_3 on the growth substrate in the presence of hydrogen and H_2S to produce MoS_2. The proof-of-concept existence of MoS_2 was demonstrated by XPS and Raman spectroscopy (Figure 11) with the stoichiometry estimated from the XPS calculated atomic percentages as $MoS_{1.4}$, which is consistent with MoS_2 formation in the absence of material- and measurement-condition-specific peak calibration. The optical images of the film show that despite the clear chemical structure the material produced on the target substrate is not a monolayer as desired but a film of particles roughly 1 µm in width.

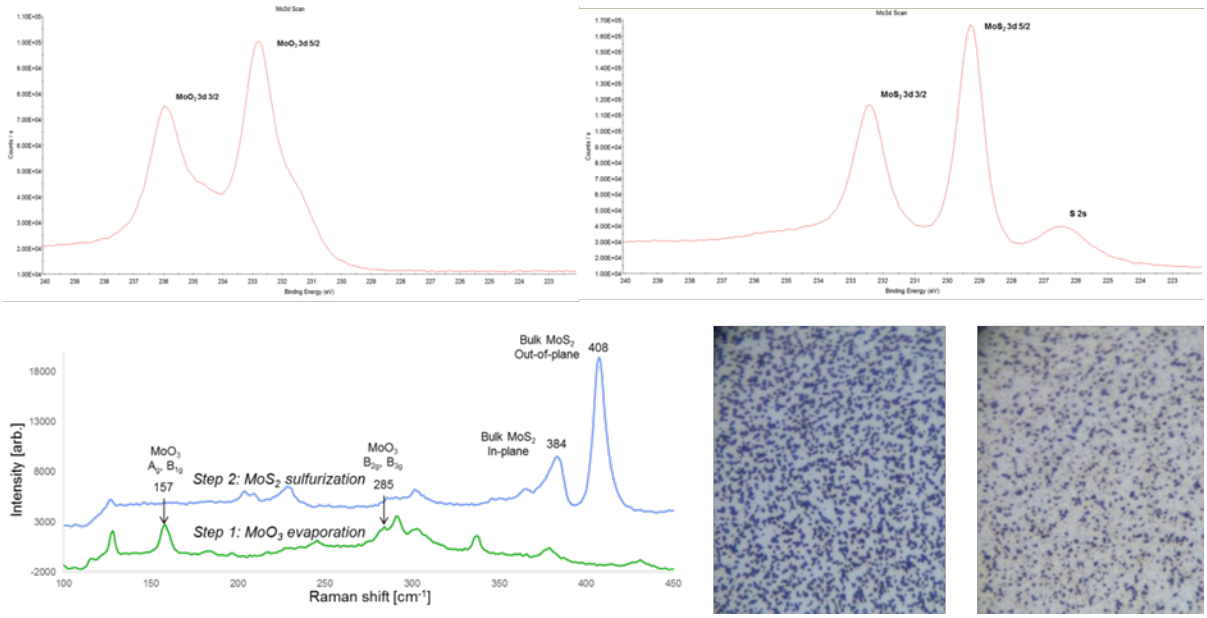

Figure 11. Characterization of the material produced by two-step TFP-VPE. (Top Left) XPS Mo3d peaks after the first MoO_3 transfer step in N_2 atmosphere. Only MoO_3 is observed on the surface. (Top Right) XPS Mo3d peaks after the second sulfurization step in the presence of H_2 and H_2S. Only molybdenum sulfide is observed on the surface. (Bottom Left) Raman spectra showing characteristic peaks for MoO_3 only after the first growth step and for MoS_2 only after the second growth step. (Bottom Center) Optical image of the MoO_3 transferred to the target wafer after the first growth step. (Bottom Right) Optical image of the MoS_2 produced on the target wafer after sulfurization of the MoO_3 in the second growth step. Vertical field of view for the optical images is 70 µm.

While the new TFP-VPE process is promising in that it produces the desired MoS_2 material, the difficulties of this approach have become apparent. Namely, the initial system design does not have the thermal control of the target wafer that is necessary to produce a uniform film, the concentration of H_2S gas is inherently nonuniform as it diffuses toward the center of the wafers from the perimeter, and the process of sulfurization completely reacts the MoO_3 source leading to use only as a single-cycle growth method (which does not allow multiple evaporation/sulfurization cycles in order to produce a smoother target film). To continue this approach to TMD growth, a separate reactor design might be employed where the target wafer is resistively heated, the source wafer is replaced by a fine mesh screen assembly through which gas may be flown to result in a constant radial gas velocity, which together address the first two issues. The third issue is less tractable while preserving the solid film precursor concept. Therefore the FY18 efforts will focus on VPE growth over TFP-VPE growth, which is considered to be more amenable to improvement of the reactor and growth process.

3.4 TEM IMAGING

To interrogate the physical properties of our WS_2 films, we employed Transmission Electron Microscopy (TEM). TEM is a powerful technique that can be used to image samples with very high resolution, and operates by the passage of an electron beam through a sample after the electrons have been accelerated through an electric potential. At a basic level, thicker areas of material will block more electrons, appearing darker upon a phosphorescent screen, whereas thinner areas will appear correspondingly lighter. Due to the much smaller wavelengths of the electrons, the image obtained is of considerably higher resolution than images obtained using an optical microscope. The image itself is known as a bright-field TEM image. Much additional information can be gleaned from a TEM by considering other interactions of the electrons with the sample. For example, when electrons pass through a sample having an ordered crystalline structure, they will be diffracted due to the minute spacing of the constituent atoms. This diffraction pattern can then be analyzed in order to determine the physical structure of the material. The diffraction pattern is readily obtained by selecting the image formed at the back focal plane of the TEM.

The particular utility of TEM in imaging 2D films is in its ability to reveal grain boundaries and defects that degrade the electronic properties of materials. The presence of grain boundaries is known to cause the scattering of charge carriers, affecting their transport in an adverse manner (i.e., decreasing the mobility). TEM can also reveal the existence of single vs. multi-layer regions of material in bright-field images, and diffraction patterns can reveal not only the presence of multi-layer areas, but their crystal structure and orientation as well.

We decided to use Aberration-corrected Transmission Electron Microscopy to image our films in addition to conventional TEM. Though considerably more difficult to accomplish, aberration-corrected TEM enables one to image sample material with much higher resolution. An additional set of lenses is incorporated into the columns of aberration-corrected TEMs in order to correct for spherical aberrations, and fine details that were previously difficult to observe become clear. Imaging our early WS_2 films confirmed the existence of monolayer regions of material, but also revealed many areas of multi-layer growth in close proximity to the single-layer areas (left-hand side of Figure 12). We found that this was true of every area of the film that we imaged, although the size and shape of the single and multi-layer regions varied. This indicated that we needed to fine-tune our growth parameters in order to avoid multi-layer growth of WS_2.

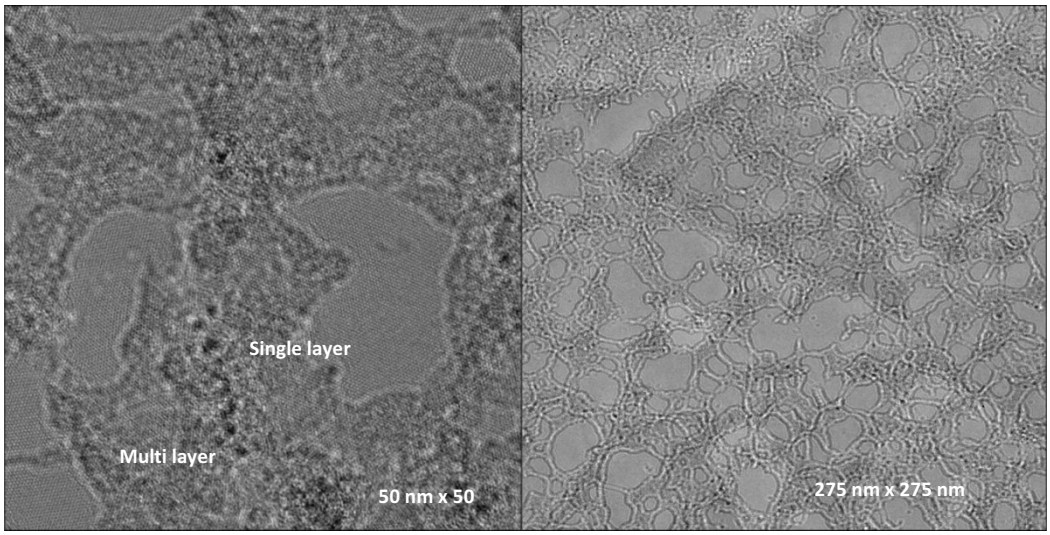

Figure 12. Aberration-corrected TEM Images of WS_2.

This page intentionally left blank.

4. DEVICE FABRICATION AND SPATIO-TEMPORALLY RESOLVED PHOTOLUMINESCENCE SPECTROSCOPY

Valleytronic materials such as two-dimensional transition metal dichalcogenides hold much promise to enable innovative forms of computation that can outperform silicon-based technology. Resolving their optoelectronic properties both spatially and temporally is an essential step toward achieving this goal. We have demonstrated device-scale growth of valleytronic material and measured exciton lifetimes on the order of nanoseconds.

4.1 INTRODUCTION

Conventional technologies based on silicon have been fast approaching the limits of scaling in recent years, and the need for other forms of computation has continued to grow. This demand is being met in part by looking to technologies based on different physics such as spintronics and quantum computing. An alternate form of computing, based on valleytronic materials, is a promising route to enable the US to maintain its dominance in the field of computation.

Valleytronic materials are typically semiconductors with valleys in their electronic band structure that can be selectively addressed. For example, ultrathin layers of transition metal dichalcogenide (TMD) materials such as monolayer tungsten disulfide (WS_2) or molybdenum disulfide (MoS_2) are suitable candidates since valleys appear in their band structure that can be selectively populated with electrons. Although energy-degenerate, the valleys are non-equivalent with regard to momentum due to the broken inversion symmetry that exists for monolayers of these materials. Thus, the valley degree of freedom can be used to enable a new form of computing that depends no longer on the charge of the electron (as with conventional transistors), but rather on its momentum and spin. Some of the advantages to this approach are thought to include improved energy-efficiency and faster speeds of computation as compared to silicon-based devices.

One way of implementing valleytronics is to selectively populate individual valleys by illuminating a sample with circularly polarized light to create valley-polarized excitons or free carriers. Remarkably, upon recombination, light is emitted with the same helicity as the incident light. When an electric field is applied to the material in a uniaxial direction, the valley Hall effect will induce transverse motion of carriers in opposite directions based on their valleys. Together these techniques provide physically-realizable mechanisms for information initialization, transport and readout.

Feasible valleytronic computing will require large-scale device fabrication and valley coherence times much longer than gate operation times. Here we address both of these issues.

4.2 WAFER-SCALE DEVICE FABRICATION

TMD materials can be grown at a large scale using the technique of chemical vapor deposition or CVD. Chemical precursors flow through a heated tubular furnace and react at a prepared substrate surface (SiO_2, sapphire, etc.) to produce the desired film. The precursor amounts, and the ratio of these amounts, are carefully controlled in order to grow the film. The temperature of the furnace, the placement of the substrate in the reactor, and the flowrate of the carrier gas are also important variables that have to be precisely controlled to achieve reproducible growths. The Kong group at MIT has grown single-layer MoS_2 up to the centimeter-scale on silicon dioxide using CVD. The material can be successfully patterned at a large-scale using optical lithography and plasma etching, as we have demonstrated in the left-hand image of Figure 13.

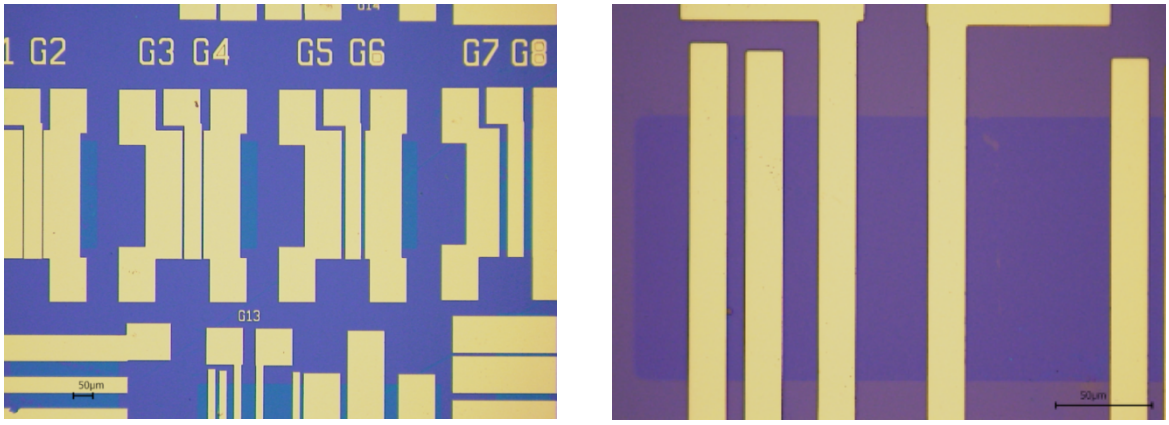

Figure 13. Large-scale MoS_2 device patterning.

A close-up of a patterned device is depicted on the right in Figure 14 (scale-bar represents 50 µm), showing that the monolayer film extends several tens of microns in either dimension after being sectioned into a rectangular area. This is an important step forward over earlier published devices which were created on small MoS_2 flakes by non-scalable e-beam lithography. These flakes were obtained using the well-established technique of mechanical exfoliation to obtain few layers of high-quality material from larger crystals. Unfortunately, the sizes of the thin layers obtained by this method are very small (some tens of microns at most), and a scalable technology cannot be established by employing this method.

Example back-gated FET characteristics of our devices are depicted in Figure 15. A mobility of approximately 0.7 cm^2/Vs and an on/off ratio of $\sim 10^6$ were observed, consistent with values typically obtained for CVD films [1]. The FETs display an over two-fold increase in the current upon illumination (not shown). This is a key result since photoconductivity under a finite bias is an essential component of the valley Hall effect [2]. Note that the low currents are due to the long channel. Here it should be emphasized that valleytronic information processing will occur in momentum space, and these FETs are

intended as characterization vehicles for material quality and device integration and are not enabling computational elements themselves.

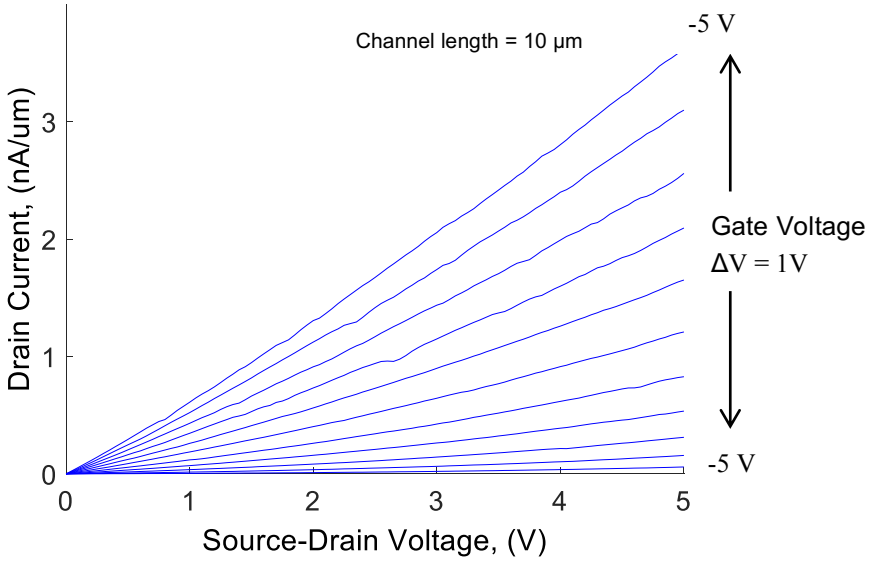

Figure 14. Back-gated MoS_2 transistor.

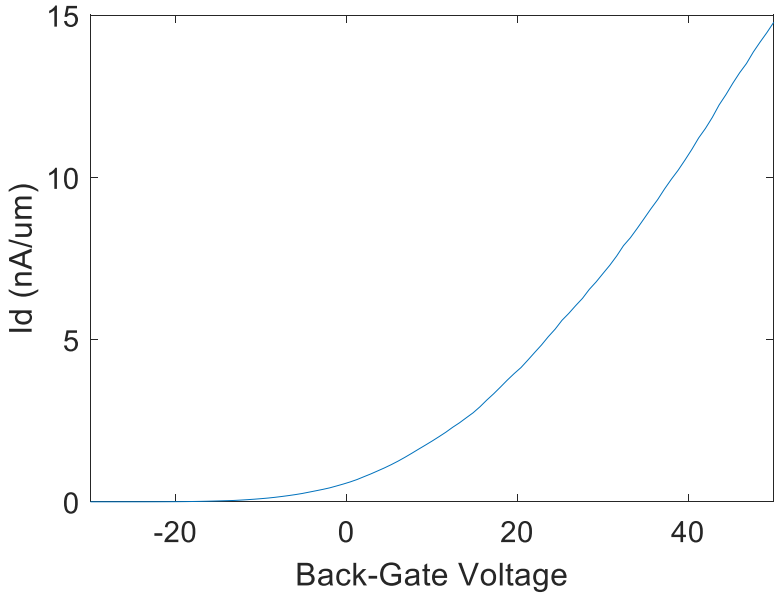

Figure 15. MoS_2 transistor transfer characteristic curve.

Figure 15 depicts the transfer characteristic curve of a back-gated transistor. The threshold voltage occurs at positive values, and we are able to observe saturation (not depicted). This is a desirable characteristic and an encouraging result not often observed in CVD-based FETs, and indicates a shift in the Fermi level away from the conduction band minimum.

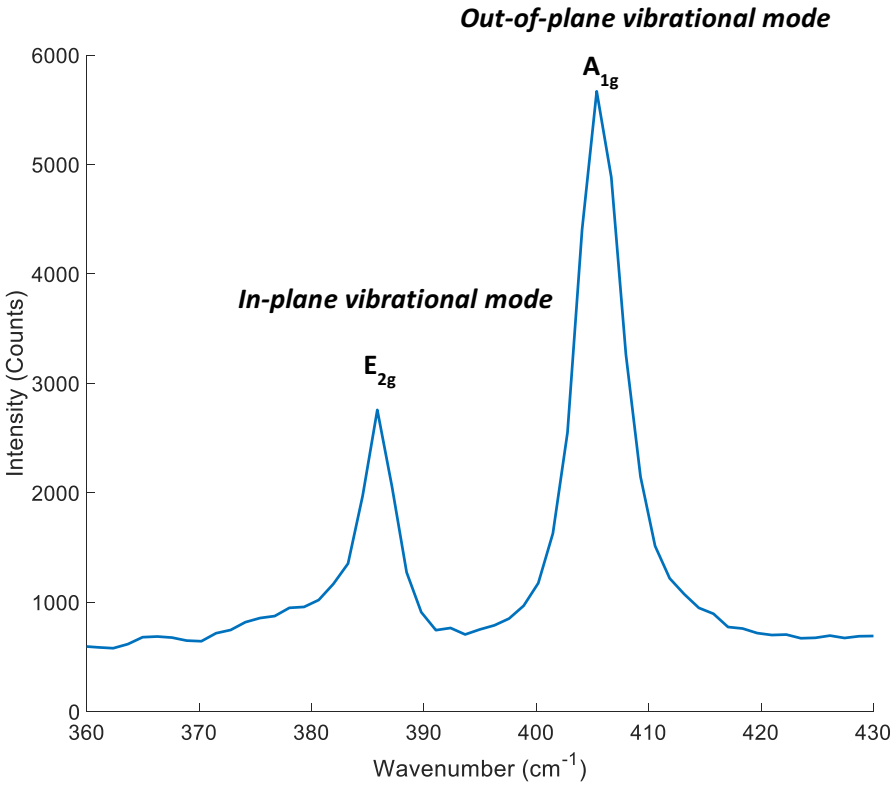

Figure 16. Raman spectrum of single-layer MoS_2.

Figure 16 shows a Raman spectrum acquired using Lincoln Laboratory's newly-installed Raman spectrometer that confirms the identity of the FET material as single-layer MoS_2. The peaks depicted in the figure correspond to different vibrational modes of the material. One mode, referred to as the E_{2g} mode, is characterized by the vibration of the atoms of the material in the plane of the sample itself. The other, referred to as the A_{1g} mode, is indicative of the out-of-plane vibrations of the atoms of the material. The vibrational modes can convey a great deal of information about the sample – first and foremost, they are highly useful in indicating the number of layers of the material. The distance between the peaks will widen as the number of layers increases. When differentiating between single layers of two-dimensional TMD materials, Raman microscopy is a powerful tool for rapidly confirming whether the material we are using for fabricating devices and spectroscopic characterization is in fact monolayer. The only other readily available technique that can reliably do so, but is far more time consuming, is atomic force microscopy.

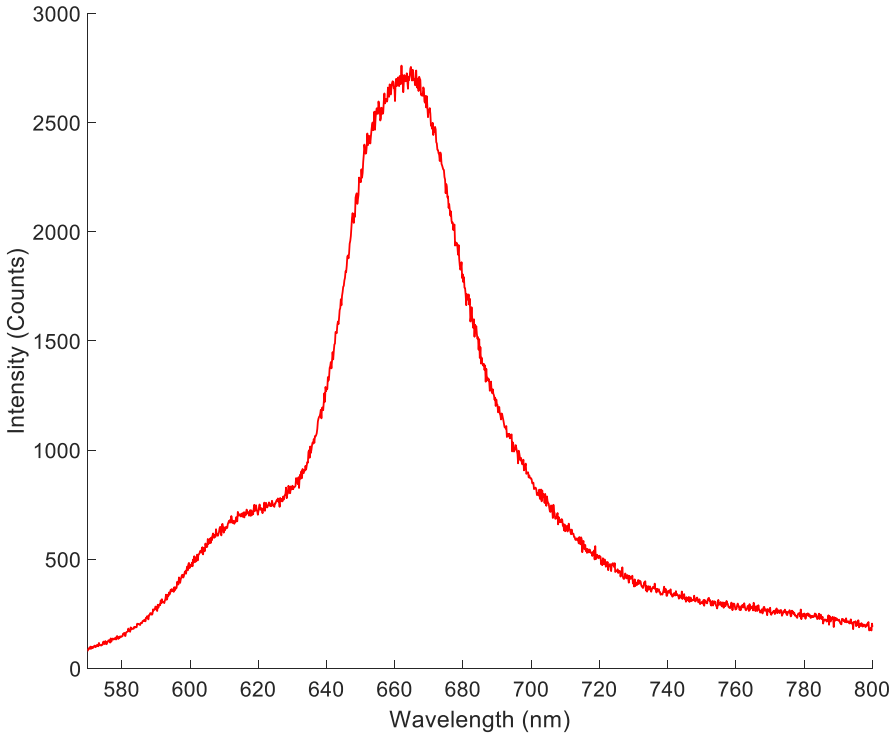

Figure 17. Single-layer MoS_2 photoluminescence.

Figure 17 depicts a photoluminescence spectrum of single-layer molybdenum disulfide. The primary peak at approximately 660 nm is due to the A excitonic transition of the material, and is characteristic of monolayer MoS_2. A smaller peak can be observed closer to 630 nm that is associated with the B excitonic transition of the material. More than one excitonic state occurs due to spin-orbit splitting of the valence band. The peaks of TMD materials can often be convolutions of more complicated excitonic states involving multiple charge carriers (trions, etc.). This can be confirmed by the use of gate voltages that can be used to split the photoluminescence peaks to reveal the existence of these exotic states.

The left-hand side of Figure 18 shows a photoluminescence map of single-layer MoS_2 that has been patterned as part of a device. The spatial map reveals variations in the intensity of the luminescence as a function of position, and gives us a powerful tool by which to characterize the properties of the material for device fabrication. The device itself (depicted on the right side of Figure 18) will allow us to investigate the electroluminescent properties of the material by the application of an in-plane voltage. We can further apply a gate voltage in order to vary the Fermi level and investigate the spatial mapping of a particular excitonic species (trion vs. exciton, etc.). We are currently pursuing this capability with the intent of correlating such opto-electronic effects with the sample temperature.

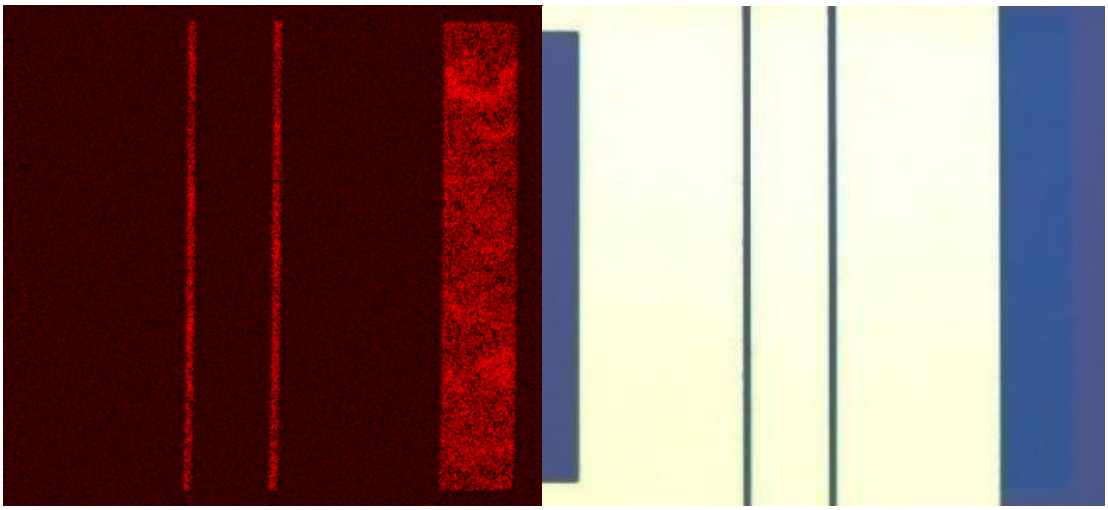

Figure 18. Spatial map of steady-state photoluminescence of single-layer MoS_2.

Figure 19 shows a qualitative measure of valley coherence. A laser beam with a wavelength of 633 nm is used to excite exfoliated single-layer MoS_2, where the wavelength is chosen in order to probe the valleys of MoS_2 (which emits light near 660 nm). The beam is circularly polarized using a quarter-wave plate in order to couple the field selectively to the carriers of the material. It is observed that the sample illuminated with circularly polarized light preferentially emits photoluminescence (PL) with the same helicity as the incident light. This demonstrates that the valley coherence time is long compared to the excitation, relaxation, and recombination processes. Though these measurements were taken at 77K, other data (not shown) suggests that valley polarization persists even up to room temperature which is critical for practical valleytronic computing.

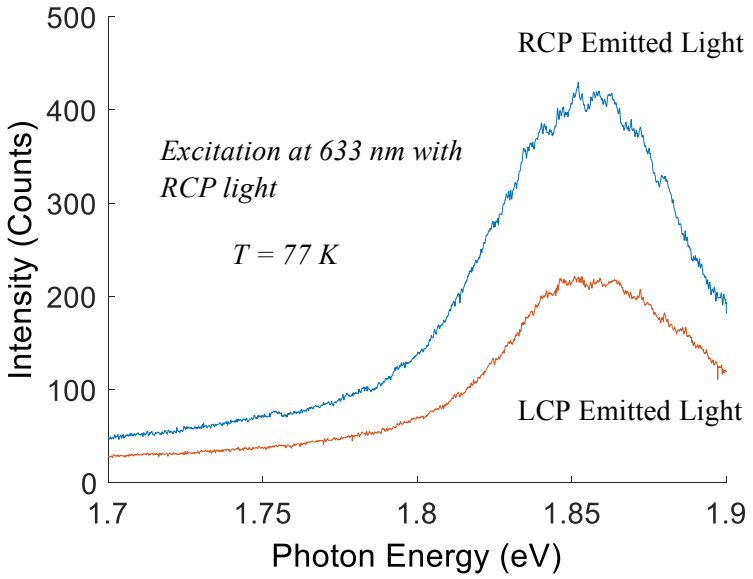

Figure 19. Valley-based photoluminescent response of single-layer MoS_2.

4.3 SPATIO-TEMPORALLY RESOLVED PHOTOLUMINESCENCE SPECTROSCOPY

A fundamental valleytronic parameter that determines the feasibility of a valleytronic devices is the coherence time. The coherence dictates the length of time during which a valleytronic computation must be executed, and is decided by how long a charge carrier will reside in a given valley before some physical mechanism causes its state to change. Unfortunately, these mechanisms often occur at extremely fast timescales (femtosecond to nanosecond) and are difficult to characterize. Time-resolved photoluminescence spectroscopy (TRPL) allows one to dynamically probe the opto-electronic properties of a material at timescales that are typically too fast to observe by other means. For example, pump-probe laser setups that are used to obtain TRPL data can routinely resolve the dynamics of a process at the femtosecond scale (10^{-15} s). This is usually done by first illuminating a sample with a pulsed laser beam (called the pump), causing a change in an optical property of the sample, which is monitored by using another pulsed beam (called the probe) which interacts with the material a short time later. The change due to the 'pump' is thus determined by the 'probe'. Though quite complex to implement in practice, it is a very powerful technique that is extremely useful both for its resolution and its ability to characterize the opto-electronic properties of a material. Falling under the category of non-linear optics. it can be used to elucidate material dynamics such as second-harmonic generation, four-wave mixing, the Kerr effect, and more. The resolution is unparalleled as it is essentially limited by the width of the light pulse, and not by the electronics of a time-resolved setup. We are currently constructing a pump-probe setup in collaboration with the Gedik group at MIT.

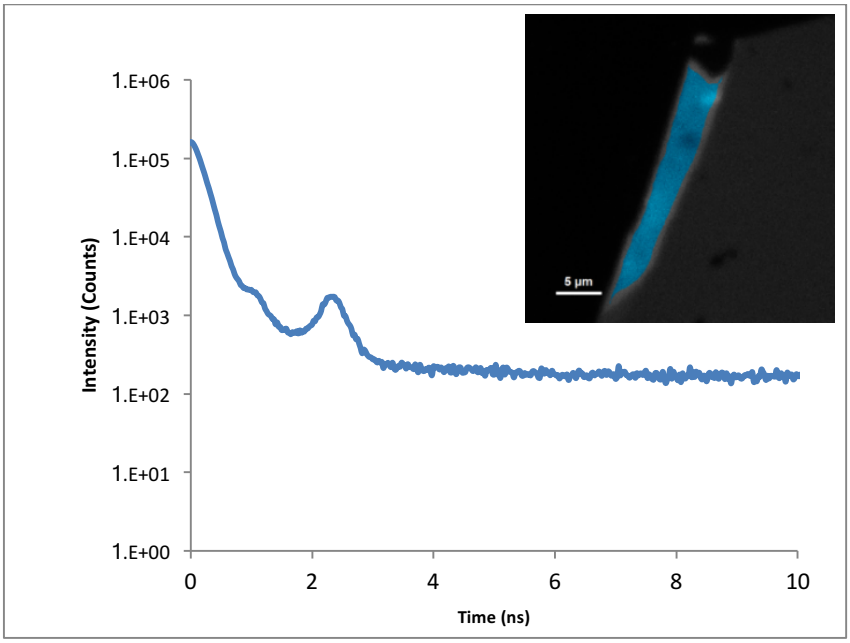

Figure 20. Single-layer MoS_2 spatio-temporal dynamics.

A time-resolved setup that probes material dynamics at longer timescales – on the order of picoseconds – is that of time-correlated single photon counting (TCSPC). A preliminary TCSPC decay curve (blue) of a single-layer MoS_2 flake obtained at room temperature is depicted in Figure 20. The acquisition parameters and multi-exponential fit (red curve; decay constants: 94 ps, 124 ps, 1.24 ns) indicate that several relaxation processes occur and that radiative and non-radiative channels likely contribute to the observed decay [3, 4]. The peaks that appear in the decay curve are reflection artifacts that have not yet been eliminated from the system. We are currently developing models to understand the specifics of these decay channels, as understanding of these channels will provide information necessary to increase valley lifetime by reducing decoherence mechanisms. The inset shows PL intensity across the sample. PL quenching near the edges is observed which suggests that increased valley coherence time requires large area valleytronic material as illustrated earlier.

A TCSPC setup that we have developed in collaboration with the Harvard University Center for Nanoscale Systems has also been used to obtain decay curves. The advantage of this setup is that we are able to modify the optics in the beam path, and are currently working to incorporate polarization optics that will allow us to illuminate the sample with circularly polarized light. We will thus be able to obtain time-resolved information with picosecond resolution that can be correlated with valley-specific effects. A decay curve of multi-layer MoS_2 obtained using this custom system is depicted in Figure 21.

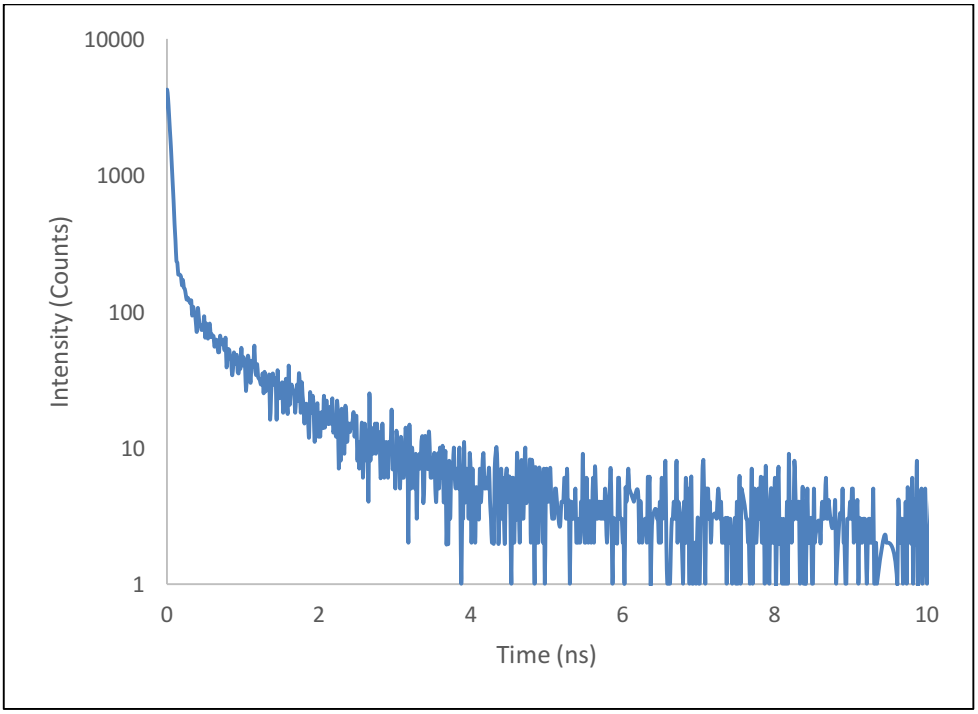

Figure 21. Custom system time-resolved decay trace.

5. PUBLICATIONS AND PRESENTATIONS

1. J.O. Varghese, S.A. Vitale, P.C. Shen, E. Ergecen, M. Yilmaz, D. Nezich, B. Burant, J. Kong, N. Gedik, and M. Rothschild, "Large-Scale Device Fabrication and Spatio-Temporally Resolved Photoluminescence Spectroscopy of Valleytronic Materials," submitted to GOMACTech-18, Miami, FL, March 2018.

2. B. Burant, "Plasma-enhanced ALD Thin Films for use in Controllable 2D Material Synthesis," AVS 64th Annual Symposium, Tampa, FL, October 2017.

3. S.A. Vitale, D. Nezich, J.O. Varghese, "Valleytronic Information Processing with 2D Materials," MIT-MTL Center for Graphene Devices and 2D Systems, Cambridge, MA, October 2017.

4. S. Vitale, "Quantum Engineering at MIT Lincoln Laboratory," CIQM Annual Meeting, Medford, MA, October 2017.

5. D. Nezich, V. Liberman, J.O. Varghese, S.A. Vitale, and M. Rothschild, "Spectroscopic Ellipsometry of Large-Area Tungsten Disulfide," 2017 MRS Spring Meeting and Exhibit, Phoenix, AZ, April 2017.

6. J.O. Varghese, D. Nezich, S.A. Vitale, M. Rothschild, "Wafer-Scale Growth of 2D WS_2 for Valleytronic Devices," GOMACTech-17, Reno, NV, March 2017.

7. S.A. Vitale, D. Nezich, J.O. Varghese, "Monolayer Valleytronic Materials," MIT-MTL Center for Graphene Devices and 2D Systems, Cambridge, MA, November 2016.

This page intentionally left blank.

6. SUMMARY

Significant progress was made in FY17, though there is still a long way to go to establish the feasibility of using the valley index for information processing. The FY17 effort was a multi-institutional program, in spite of the fact that no funding was sent by Lincoln Laboratory to other institutions. Collaboration with the Harvard Center for Nanoscale Science allowed us to modify one of their instruments to measure the PL properties of Lincoln-Laboratory-grown WS_2 and compare it to exfoliated MoS_2 samples, which provided important feedback on the WS_2 growth process. Demonstration of valley polarized emission from MoS_2 at 77 K and room temperature confirms that valleytronic effects persist at room temperature, which is key for some applications. Our first measurements of PL lifetime were performed in collaboration with the Harvard Center for Biological Imaging. These measurements demonstrated the feasibility of performing spatially-resolved mapping of micron-scale domains of monolayer material, and provided the first indications of how edges influence exciton lifetime.

At MIT, we began construction of a femtosecond pump-probe valley spectroscopy system in collaboration with Prof. Nuh Gedik. The system is still under construction, but we expect we will use it to perform the first spatially-resolved study of fs valley dynamics shortly. Also at MIT, Prof. Jing Kong's group provided samples of CVD-grown monolayer MoS_2. Working together with that group we fabricated micron-scale transistors which gave us our first direct measurements of the carrier transport properties in this material. A third collaboration with MIT was initiated with Prof. Jeehwan Kim. Prof. Kim was able to perform a layer-resolved transfer technique on Lincoln-Laboratory-grown WS_2. By peeling off individual monolayers of material from our multilayer samples, we were able to observe how the material quality improves layer-by-layer, form the substrate to the top layer. This again is important feedback for optimizing the growth process.

At Lincoln Laboratory, we made progress in both the material growth and spectroscopy technical areas. Domain size of our VPE-grown WS_2 increased from 0.1 um to 2.2 um through process optimization. This is extremely important as valleytronic properties are expected to increase in direct proportion to domain size. A variation on this process which we have termed thin-film precursor VPE was developed to improve the across wafer uniformity of the growth process. PL and Raman measurements show this technique has promise to grow useful MoS_2 material, though the domain size has not yet been measured. Construction of a low pressure VPE growth system here at Lincoln Laboratory is nearly complete. This system will provide access to new regimes of mass transport and surface kinetics which we think will allow order of magnitude increase in domain size. In the spectroscopy area, Lincoln Laboratory was lacking the basic tools necessary to perform materials characterization. This year we were able to acquire and install two important pieces of capital equipment through Division 8 financial support (not Line) which are crucial to our FY18 efforts. First is a commercial Raman microscope that we will modify to perform valley polarization experiments. Second is a 4 K closed-cycle cryostat, which will be integrated with the Raman microscope. Measurements from cryogenic to room temperature will allow us to look at the activation

energy of different polarization loss mechanisms in these materials and hopefully to correlate these mechanisms with specific material defects.

Our most multi-institutional activity for FY17 was the organization of the Valleytronics Materials, Architectures, and Devices Workshop. Lincoln Laboratory, MIT, and Harvard co-organized the workshop; in addition, the National Science Foundation provided financial support and guidance. We are very pleased that over 60 leading researchers attended our workshop. We learned a great deal about the state of the art in valleytronics, as well as the opportunities and challenges going forward, much of which has been provided in this report.

Finally, we are pleased that our work has been accepted for presentation at a number of conferences as listed in the "Papers and Presentations" section.

Looking forward to FY18, we intend to address some of the key risks associated with using the valley index as a means of information processing. Foremost is the development of an architecture which provides theoretical power or performance advantage over the state of the art. This will be another collaborative effort with MIT. We will continue our experimental collaboration with Prof. Gedik to determine the effect of power density, and excitation wavelength on spatially-resolved valley lifetime of MoS_2, while comparing CVD and exfoliated material to understand how defects present in each growth method influence the dynamics. At Lincoln Laboratory, we will examine the kinetics of polarization through temperature- and spatially- resolved measurements. Our modified VPE system will demonstrate growth in the low-pressure regime and optimize growth for large domain size. We will continue the collaboration with Prof. Kim to get feedback on our growth process.